

Chapter 5

Changes in Canadian Arctic Ice Shelf Extent Since 1906

Derek Mueller, Luke Copland, and Martin O. Jeffries

Abstract The ice shelves along the northern coast of Ellesmere Island have been in a state of decline since at least the early twentieth century. Available data derived from explorers' journals, aerial photographs and satellite imagery have been compiled into a single geospatial database of ice shelf and glacier ice tongue extent over 13 observation periods between 1906 and 2015. During this time there was a loss of 8,061 km² (94%) in ice shelf area. The vast majority of this loss occurred via episodic calving, in particular during the first six decades of the twentieth century. More recently, between 1998 and 2015, 515 km² of shelf ice calved. Some ice shelves also thinned *in situ*, transitioning to thinner and weaker ice types that can no longer be considered ice shelf, although the timing of this shift is difficult to constrain with the methods used here. Some ice shelves composed partly of ice tongues (glacier or composite ice shelves) also disintegrated to the point where the ice tongues were isolated, representing a loss of ice shelf extent. Our digitization methods are typically repeatable to within 3%, and generally agree with past determinations of extent. The break-up of these massive features is an ongoing phenomenon, and it is hoped that the comprehensive dataset presented here will provide a basis for comparison of future changes in this region.

Keywords Ice shelf • Ice tongue • Break-up • Calving • Climate change • Change detection • Remote sensing • Geographic Information System (GIS) • Arctic

D. Mueller (✉)

Department of Geography and Environmental Studies, Carleton University,
Ottawa, ON, Canada

e-mail: derek.mueller@carleton.ca

L. Copland

Department of Geography, Environment and Geomatics, University of Ottawa,
Ottawa, ON, Canada

e-mail: luke.copland@uottawa.ca

M.O. Jeffries

Office of Naval Research, Arctic and Global Prediction Program, Arlington, VA, USA

e-mail: martin.jeffries@navy.mil

5.1 Introduction

Historical losses of the Ellesmere Island ice shelves in Nunavut, Canada, have been documented in many previous articles and reports. Most of these are concerned with a particular calving event, or events, between sporadic field or remote sensing observations (Hattersley-Smith 1963, 1967; Jeffries 1982, 1986a, 1992b; Jeffries and Serson 1983; Jeffries and Sackinger 1991; Vincent et al. 2001, 2009, 2011; Mueller et al. 2003; Copland et al. 2007). Some have focused on the changes that have occurred to a particular ice shelf over time (Copland et al. 2007; Pope et al. 2012; White et al. 2015), while others have described the extent of all the Ellesmere ice shelves at once (Mueller et al. 2006). In addition, some articles have calculated the past extent of all ice shelves and compared them to various points in history (Vincent et al. 2001) or examined the extent lost during calving events (Jeffries 1987, 1992a). Despite this work, there has not yet been a comprehensive and rigorous analysis of the change in all the Ellesmere Island ice shelf extents over the entire record of available satellite remote sensing, aerial photograph and anecdotal data.

The ice shelves along the northern coast of Ellesmere Island were formed by a combination of multiyear landfast sea ice accretion and glacier input followed by thickening via snow accumulation (Dowdeswell and Jeffries 2017). The ice shelves are thought to be several thousand years old (Antoniades 2017; England et al. 2017) and are characterized by an undulating surface (Jeffries 2017). Multiyear landfast sea ice may also have these surface features, but with a closer spacing, which is thought to relate the thinner nature of this less-developed ice type. Ice shelves were known to occupy the mouths of embayments and fiords along the northern coast of Ellesmere Island. This often leaves an area of relatively thin freshwater ice between the head of the fiord and the ice shelf. This situation, known as an epishelf lake, is caused by the impoundment of a fresh meltwater layer by the ice shelf that lies atop denser seawater beneath (Veillette et al. 2008; Jungblut et al. 2017). Over the last decade there has been a dramatic loss of ice shelves, multiyear sea ice and epishelf lakes (Mueller et al. 2003; Copland et al. 2007; Veillette et al. 2008; Pope et al. 2012, 2017; White et al. 2015).

The purpose of this chapter is to review available information on the extent of the Ellesmere ice shelves and to refine the timing of calving events between 1906 and 2015. We lay out a series of methodological principles for quantifying ice shelf extent and change, and use geospatial data and Geographic Information System (GIS) techniques to accomplish this. This chapter also discusses issues related to the available data and their interpretation. The underlying data compiled for this project include maps generated from explorers' journals, maps created from air photographs, as well as optical and radar remote sensing imagery of various resolutions and polarizations. The temporal resolution of observations increases over time and increasingly over the past two decades it has been possible to obtain excellent satellite coverage of the northern coast of Ellesmere Island on a regular basis. The limitations of each method and the challenges of combining them are evaluated.

This chapter provides a description of temporal changes in ice shelf extent, but does not attempt a detailed explanation of their causes as this is covered by other chapters in this book (e.g., Copland et al. 2017). The geospatial data that were produced from the analyses conducted for this chapter are published separately (Mueller et al. 2017) and the metadata is accessible online (<http://polardata.ca/12721>), so that others can study and improve on them, but the underlying imagery remain with the copyright holder or, in some cases, on separate online repositories.

5.2 Methods

The collection of data proceeded as follows: each data source (Sect. 5.2.1; Table 5.1) was converted to an electronic format by scanning, if it was not already available as a digital image. Data sources (Sect. 5.2.1) were georeferenced or a correction to the existing georeferencing was applied (Sect. 5.2.2). Digitizing of each feature followed a protocol (Sect. 5.2.3), and data were cleaned and verified (Sect. 5.2.4). Following data entry, data display and analysis were conducted.

Table 5.1 Data sources by observation year and season

Year	Season	Sources	Data type	Notes
1906	Summer	Vincent et al. (2001), Bushnell (1956)	Anecdotal/survey	
1959	Summer	NTS maps; Aerial photos	Aerial photo/map	
1963	Summer	Corona	Optical satellite	Snow-covered, difficult to discern ice types
1988	Summer	SPOT-1	Optical satellite	Missing east of central Ward Hunt Ice Shelf
1992	Winter	ERS-1	SAR satellite	Missing east of western Ward Hunt Ice Shelf
1998	Winter	RADARSAT-1	SAR satellite	Hard to see fragments in Ayles Fiord
2003	Winter	RADARSAT-1	SAR satellite	
2006	Winter	RADARSAT-1	SAR satellite	
2009	Winter	RADARSAT-1	SAR satellite	
2011	Winter	RADARSAT-2	SAR satellite	
2012	Winter	RADARSAT-2	SAR satellite	
2013	Winter	RADARSAT-2	SAR satellite	
2015	Winter	RADARSAT-2	SAR satellite	

5.2.1 Data Sources

Four main data types were used to examine ice shelf extent along the northern coast of Ellesmere Island: anecdotal reports and survey data; aerial photographs and published maps; optical satellite remote sensing and synthetic aperture radar (SAR) satellite remote sensing. These vary substantially with respect to accuracy, as well as spatial and temporal coverage. As described below, we used each of the data types in succession and prioritized observation years that had the greatest spatial coverage. This meant that some datasets were not incorporated into the analysis due to restricted spatial coverage (e.g., aerial photographs from 1974 and 1987, and airborne real aperture radar from the 1980s) or, in later years, because of the availability of imagery with a high temporal frequency that did not show significant changes between scenes. When possible, imagery with the highest spatial resolution and accuracy was prioritized and observation years were selected to bracket major calving events.

5.2.1.1 Anecdotal/Survey

The first documented visit to the ‘Ellesmere Ice Shelf’ (unofficial name) was in 1876 by a sledge party led by Lieutenant Pelham Aldrich as part of the British Arctic Expedition (Aldrich 1877; for selected quotes see Copland et al. 2017). Aldrich described travelling over ice shelf ice, but a subsequent visit by Commander Robert Peary in 1906 yielded more precise descriptions of the ice type and he explored further along the coast than his predecessor (Peary 1907; for selected quotes see Jeffries 2017). Therefore, anecdotal evidence in Peary’s journal was used to map the extent of the ice shelf from Cape Hecla to the northern end of Axel Heiberg Island (Fig. 5.1) by Vincent et al. (2001). This estimation assumed that the northern edge of the ice shelf went from headland to headland and that shelf ice filled the outer portion of bays and fiords along the coast. From Cape Richards to Point Moss (adjacent to ice shelves that bear these names; Fig. 5.1), the northern limit of the ice shelf was determined by the position of ocean depth soundings by Peary’s compatriot, Ross G. Marvin. He travelled along the edge of the ice shelf and his sightings of mountains along the coast were used to fix his position by triangulation (Bushnell 1956). This information was also incorporated by Vincent et al. (2001), and Fig. 2 in Bushnell (1956) was used as a data source for the ice shelf front in this study.

5.2.1.2 Aerial Photographs/Maps

In 1959 and 1960, the first complete vertical (nadir) aerial photography of the region was conducted by the Royal Canadian Air Force and topographic maps were published based on photogrammetry of this data source. Scans of the printed 1:250,000

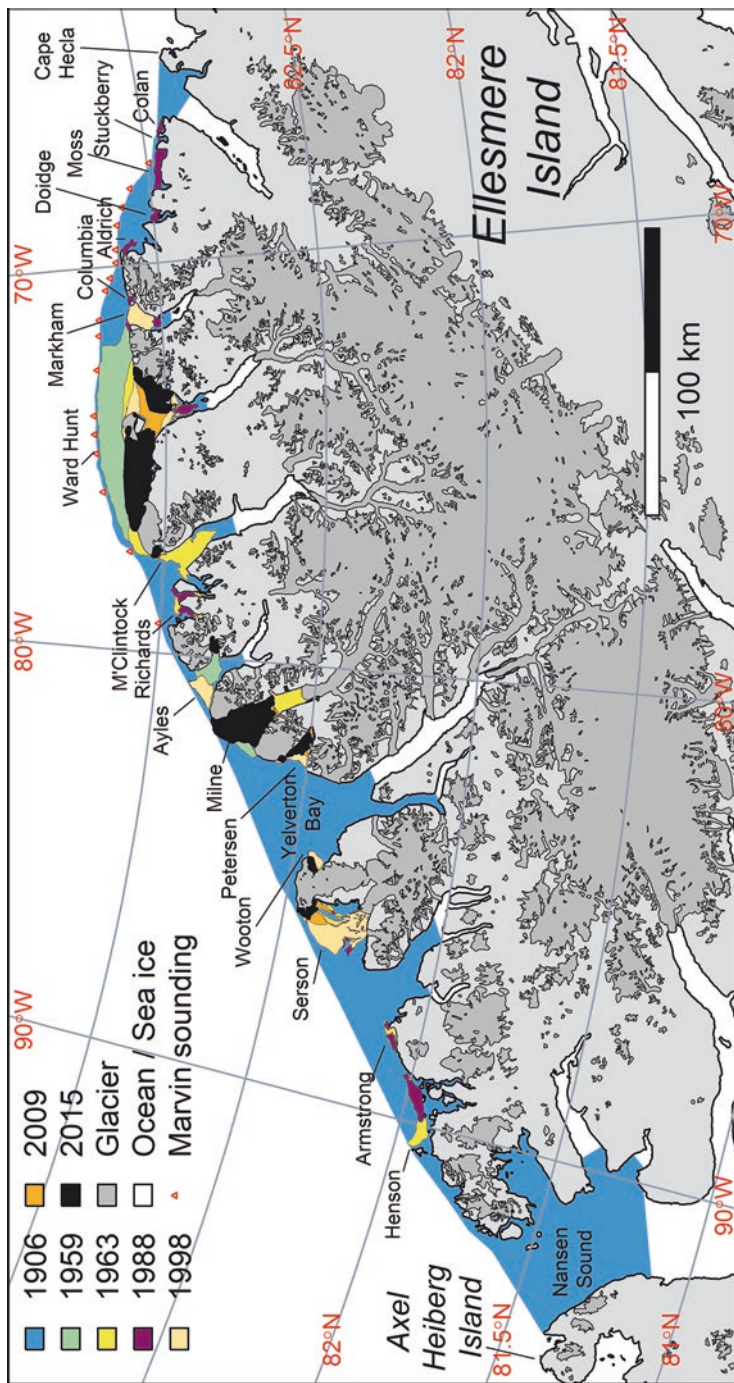


Fig. 5.1 Ice shelf extent for selected years from 1906 to 2015 in the study area. The ice shelves from the mid-twentieth century are labeled from west to east: Henson*, Armstrong*, Serson**, Wootton*, Petersen*, Milne†, Ayles†, Richards*, M'Clintock†, Ward Hunt†, Markham*, Columbia*, Aldrich*, Doidge*, Moss*, Stuckberry* and Colan* ice shelves (†official name; *formerly-known as Alfred Ernest Ice Shelf; ‡named unofficially in previous literature; †named unofficially for the first time herein). The colours indicate the year when each extent was last observed, but note that the extent from more recent years cover the extent of previous years. The 1906 extent (all non-grey and white regions) is the Ellesmere Ice Shelf. A portion of the northern edge of this large ice shelf was surveyed by Ross Marvin (red triangles; Bushnell 1956). The most recent extent is represented by black

scale National Topographic System (NTS) map sheets (120F, 340E, 340F, 560D) were used in this study, since the ice shelf feature type is not available in the published digital versions of these maps. One of these maps (340F) was erroneously constructed with some earlier aerial (trimetrogon) photographs that were acquired at select locations along the coast. As a consequence, the extent of the Serson Ice Shelf on the map reflects its extent in 1950 (Jeffries 1992b). We created a mosaic from the aerial photographs from the National Air Photo Library (Ottawa, Canada) that should have been used to create the map. This layer supplemented the map to ensure that the 1959 ice shelf extent was captured as accurately as possible.

5.2.1.3 Optical Remote Sensing

We obtained a declassified image of the northern coast of Ellesmere Island taken in 1963 by the U.S. reconnaissance satellite Corona. The Corona system involved taking photographs from low Earth orbit with 70 mm film and then releasing the undeveloped negatives to re-enter the Earth's atmosphere in a capsule for airborne retrieval (Ruffner 1995). The photographs were scanned at high resolution (90 m pixel spacing) and released to the public in 2004. A series of ten Level 2A, panchromatic SPOT 1 (Satellite Pour l'Observation de la Terre) images, covering the northern coast of Ellesmere Island in 1988, was obtained in 2014 from SPOT Image Corporation.

5.2.1.4 Synthetic Aperture Radar

From 1992 to 2015, we relied on spaceborne synthetic aperture radar (SAR) imagery. SAR is routinely used for ice discrimination and offers several advantages over optical imagery. SAR can operate through the polar night, can penetrate clouds and snow cover and is available on polar-orbiting satellites, which offer excellent acquisition possibilities (e.g., Flett 2003; De Abreu et al. 2011). Once SAR imagery was available from 1992 onwards, this image type was used exclusively to avoid mixing image types and any associated biases which can arise due to ice type discrimination. Numerous scenes were provided to us via data grants, through government collaboration and public repositories, and via organizations such as the Canadian Ice Service and Canadian Space Agency. SAR imagery from mid-winter typically provides the best contrast between ice types due to the absence of liquid water, so use of this imagery was preferred (Mueller et al. 2006; De Abreu et al. 2011). Following melt onset, the SAR backscatter signal is reduced due to absorption of microwave energy by liquid water in the overlying snow cover or on the ice surface itself, which makes it more difficult to distinguish ice types (Onstott and Shuchman 2004; Shokr and Sinha 2015). A collection of available SAR images was searched to identify candidate images that covered the ice shelves within the study area during winter (January to April). Years with complete or near complete coverage of all the ice shelves were prioritized, as were images with the highest possible spatial resolution and the most image bands.

SAR data included imagery from C-band (frequency: ~5.4 GHz, wavelength ~5.6 cm) satellites ERS-1 (European Remote-Sensing Satellite-1), RADARSAT-1 and RADARSAT-2 at a variety of spatial resolutions and polarizations (Table 5.2). The SAR scenes were provided at a smaller pixel spacing than their spatial resolution due to oversampling (Table 5.2). ERS-1 transmitted radar waves with vertical polarization and its receive antenna was likewise sensitive to vertically polarized backscatter (VV polarization). RADARSAT-1 transmitted and received in horizontal polarization (HH), whereas RADARSAT-2 is capable of transmitting and receiving in both H and V and can produce separate bands including co-polarized SAR (HH or VV), cross-polarized SAR (HV or VH) or quad-polarized SAR (HH, VV, HV and VH). Single band SAR images were analysed in grey scale, dual band images were false-coloured (Red: HH, Green and Blue: HV) prior to analysis, and quad-polarized images were converted to a Pauli Decomposition (Red: $HH - VV$, Green: $(HV + VH)/2$, Blue: $HH + VV$), which can be interpreted as the contribution made by the ice targets to single-bounce, volume and double-bounce scattering mechanisms, respectively (Lee 2009).

5.2.2 Georeferencing and Projections

To minimize distortion over the study area we used an Albers equal area projection based on the WGS-84 ellipsoid with standard parallel latitudes at 82°N and 83°N and an origin at 82°N, 75°W (<http://spatialreference.org/ref/sr-org/7968/>). A vector coastline layer was derived from the water body layer provided in the 1:250,000 National Topographic Data Base (NTDB) dataset for NTS map sheets 120F, 340E, 340F, 560D published in May 2009 (with a stated positional accuracy of 58–68 m). The NTDB data set was created from the original NTS map sheets (based on air photographs from 1959) and updated with Landsat and RADARSAT-1 imagery until 2004. This coastline served as a fixed reference throughout the project. Each satellite image was examined at a scale of 1:40,000 against this coastline to assess the quality of the original georeferencing. If the image deviated from the coastline, it was translated by an x- and y-offset to visually optimize a fit. This method was adequate to correct the georeferenced satellite imagery because the ice features are essentially at sea level and orthorectification issues can be ignored. In addition, shifting of the scenes meant that there was no need to further resample the imagery.

Depending on the incidence angle of the SAR images, there were substantial local effects from shadow or layover (an increased amount of backscatter that is a local artifact in front of steep slopes). Following image translation, deviation from the coast in areas where this could be assessed with confidence was at most 150 m (typically in the low resolution ScanSAR imagery; representing 2–3 pixels). For data acquired before the 1980s, a more sophisticated georeferencing method was employed, which used several control points along the coastline vector layer described above and an affine or polynomial transformation. For example, sections

Table 5.2 Data sources used to digitize ice shelves, ice tongues and fragments. Where more than one image/map was available on a single date, the number of images used is indicated by a superscript after the beam/mode

Platform	Date/time	Beam/mode/frame	Resolution (m)	Source
Survey	Summer 1906	NA	NA	Bushnell (1956)
Anecdotal	Summer 1906	NA	500 ^a	Vincent et al. (2001)
Map	1959-08-18	Map ⁴	50 ^a	NTS
Aerial photo	1959-07-29	A16760-90	2	NAPL
	1959-08-18	A16760-91	2	NAPL
	1959-08-18	A16760-92	2	NAPL
	1959-08-18	A16841-19	2	NAPL
	1959-08-18	A16841-21	2	NAPL
Corona	1963-08-29	Corona	110	USGS
SPOT-1	1987-08-12	Beam 1 ⁵	10	SPOT Image Corp.
ERS-1	1992-01-24	Standard	27	ASF
	1992-01-29	Standard	27	ASF
	1992-03-16	Standard	27	ASF
	1992-03-23	Standard	27	ASF
Radarsat-1	1998-01-13	ScanSAR	100	ASF
	1998-04-19	ScanSAR	100	ASF
	2003-01-07	Standard-1	27	ASF
	2003-01-11	ScanSAR	100	ASF
	2006-01-13	Standard-1	27	ASF
	2006-01-14	Standard-1	27	ASF
	2006-01-15	Standard-1	27	ASF
	2006-01-16	Standard-1	27	ASF
Radarsat-2	2009-01-04	ScanSAR	160	ASF
	2009-04-26	ScanSAR	160	ASF
	2011-01-01	ScanSAR	160	SOAR-E
	2011-01-03	ScanSAR	160	SOAR-E
	2011-02-28	Fine 21f	10	SOAR-E
	2011-03-19	Fine 2n	10	SOAR-E
	2011-03-23	Fine 5n	10	SOAR-E
	2011-04-25	Ultra-Fine 78	3	SOAR-E
	2012-02-03	Ultra-Fine 3w ²	3	SOAR-E
	2012-02-05	ScanSAR	160	CIS
	2012-02-08	Ultra-Fine 10w ²	3	SOAR-E
	2012-02-19	ScanSAR	160	CIS
	2012-03-22	Ultra-Fine 3w ²	3	SOAR-E
	2012-04-17	Fine Quad 19w	8	SOAR-E
2012-04-18	Fine Quad 21w	8	SOAR-E	
2013-03-12	ScanSAR	160	CIS	
2013-03-16	ScanSAR	160	CIS	
2013-04-27	Fine Quad 13w ²	8	CIS	

(continued)

Table 5.2 (continued)

Platform	Date/time	Beam/mode/frame	Resolution (m)	Source
	2013-04-29	Fine Quad 10w ²	8	CIS
	2013-04-30	Fine Quad 11w	8	CIS
	2015-03-22	ScanSAR	160	CIS
	2015-03-23	Fine Quad 5w	8	CIS
	2015-03-23	Fine Quad 16w	8	CIS
	2015-03-24	Fine Quad 9w	8	CIS
	2015-03-26	Fine Quad 10w ²	8	CIS
	2015-03-27	Fine Quad 15w ²	8	CIS

Sources include: National Topographic Service of Canada (NTS), National Air Photo Library (NAPL), United States Geological Survey (USGS), Alaska Satellite Facility (ASF), Canadian Space Agency's Science and Operational Applications Research – Education (SOAR-E) program and the Canadian Ice Service (CIS)

^aThese resolutions were set arbitrarily to provide a comparable error estimate to other data sources. See text for further details

of the 1:250,000 scale map sheets were georeferenced to a positional root mean square error (RMSE) of 64 m or better and the aerial photographs used for the Serson Ice Shelf had an RMSE of 71 m. The Corona image was georeferenced with 26 control points to yield a RMSE of 1331 m. Ross Marvin's soundings and the ice shelf front in 1906 from Bushnell (1956) had an RMSE of 670 m after correction using 31 control points.

5.2.3 Ice Feature Identification

The study area was defined as the region covered by ice shelves in 1906 as determined by Vincent et al. (2001; Fig. 5.1). For each observation year listed in Table 5.1, the extent of ice features was digitized offshore of the coastline vector layer. Identification and delineation of the ice types was performed at a scale of 1:25,000 using the visual cues provided by the data at hand, reports from the literature, personal communication with other experts and field knowledge. The following ice features were identified for each image date since they represent the primary forms of thick floating ice in the study area and are reasonably easy to distinguish:

Ice Shelf Ice shelves are defined as thick (≥ 20 m) and extensive landfast ice features (Dowdeswell and Jeffries 2017). Note that the thickness criterion cannot be directly evaluated with the imagery we used, although the undulating surface morphology common to all Ellesmere ice shelves (Fig. 5.2; Hattersley-Smith 1957; WMO 1970; Jeffries 2002) and field observations (if available) made them readily distinguishable from other ice types (e.g., glacier ice, multiyear landfast sea ice, first year sea ice and freshwater ice). Since we are concerned with an accounting of the changes in ice shelf extent over time we do not set a lower limit on the extent of an ice shelf.

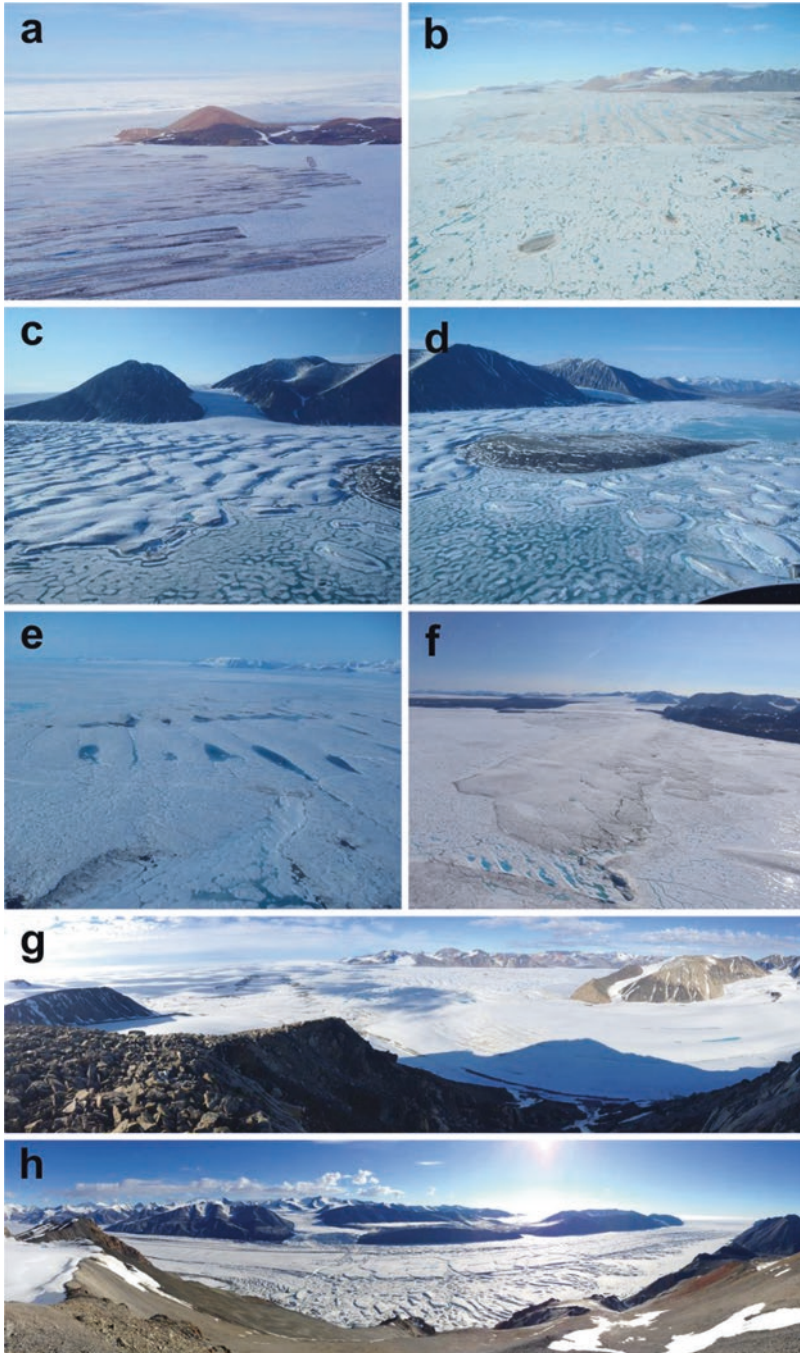


Fig. 5.2 Recent oblique photographs of selected ice features. (a) The easternmost portion of the Ward Hunt Ice Shelf south of Ward Hunt Island and ice rise. The distance to the coast of Ward Hunt Island is approximately 5 km. (18 July 2015, courtesy of A Culley); (b) Ward Hunt East Ice Shelf looking to the east. The distance from the ice shelf edge to the coast is approximately 8 km (18 July

We do not distinguish between glacial, sea-ice and composite ice shelves, the three main types of Ellesmere ice shelves defined by Lemmen et al. (1988). Grounded sections of ice shelves, known as ice rises, were excluded from the ice shelf extent. These were delineated using the coastline vector layer described above. This represents a ‘best guess’ of the true grounding line and in some cases the coastline was modified based on calving front retreat (see below).

Ice Tongue This is defined as the floating extension of a single valley glacier over the ocean. Ice tongues were considered distinct from ice shelves if they simply abutted against them. If they were incorporated into ice shelves and provided a source for them, this ice was considered to be ice shelf (e.g., northern margins of Petersen Ice Shelf; White et al. 2015). Glacier ice typically has characteristic surface flow features (e.g., medial moraines) and typically high-freeboard edges that are apparent in the imagery we analyzed. Only ice tongues within the study area that were $\sim >2$ km wide and had (at least at one point in time) an apparently extensive floating section were digitized and our analysis focuses on ice tongues that were at one time associated with ice shelves.

Ice Shelf/Tongue Fragments These are relatively small (typically <1 km²) free-floating ice features that broke away from ice shelves and ice tongues but remained within the bays and fiords that contain parent ice masses. These are essentially ice islands that have not drifted away from the study area. Their provenance is not always apparent and was not tracked.

Several principles were applied to maintain a consistent definition of the ice types and their outlines between data sources:

- (a) The coverage of each ice type was mutually exclusive, so that no two ice types occupy the same space at the same time.
- (b) Ice features were considered to be distinct when it was clear that they were separated by a substantial distance (at least 50 m) from each other following calving. Break-up (*in situ* fracturing) of ice features was not recorded explicitly due to the lack of sufficient remotely sensed data. When ice shelves disintegrated into more than one ice shelf, the largest portion retained the original name, smaller ice shelves that did not already have a name were named after their position (e.g., Ward Hunt East Ice Shelf). Non-landfast pieces that calved from ice shelves and ice tongues were considered to be ice shelf/tongue fragments.

←
Fig. 5.2 (continued) 2015, courtesy of WF Vincent); (c) The western side of the Petersen Ice Shelf (29 June 2012); (d) The inner portion of Petersen Bay showing the Petersen Ice Shelf in the background and fragments from the Petersen South Glacier ice tongue in the foreground. The island in the centre of the bay is 1.5 km long (29 June 2012); (e) Wooton (foreground) and Wooton East (behind) ice shelves with Yelverton Bay in the background. For scale, the undulating ice shelf ice in the photo is approximately 3 km along the line of sight (29 June 2012); (f) The Serson Glacier ice tongue with fragments in the foreground. The ice tongue is 7 km long (13 July 2015); (g) Panorama of the Milne Ice Shelf looking east from the west side of the fiord. The tributary glacier in the foreground merges with the Central Unit of the ice shelf. The fiord is 6.5 km wide at this point (17 July 2014); (h) Panorama of the Milne Glacier ice tongue looking west near the grounding line. The fiord is 5 km wide at this point and the detached portion of the ice tongue is 14.8 km long. (16 July 2014)

- (c) In observation years when there was no available imagery or when ice type delineation was not possible for a given ice feature (e.g., a snow-covered optical image or poor quality SAR image), the feature was assumed to persist intact. In this case, the extent digitized from the previous observation was copied to the observation year in question. If, however, there was no previous observation or there was evidence that a given calving event occurred prior to or after the missing observation year, then the extent digitized from the closest available observation year was copied to the observation year with missing data. In 1906, due to lack of evidence to the contrary, all ice tongues were assumed to be fully merged with the ice shelf.
- (d) The image used to digitize each feature was recorded in the metadata. In the case where two images were used in a digitization, due to incomplete coverage or for supplementary ice interpretation, the reference images were recorded in order of importance (i.e., the image that covered most of the feature or, in the case of a change in extent, the imagery that indicated that change, when part of the feature was missing).

The 2009 coastline vector consistently deviated from the coastline observed in imagery in a few places. This was due to errors introduced in the generation of the original map (and the NTDB data set that the map was based on), as well as the loss of ice rise and glacier ice after 1959. In these cases, it was necessary to delineate ice types on the landward side of the 2009 coastline. In the case of undefined coastlines such as at the calving front of ice tongues, the minimum extent of the ice cover over the study period was taken as the coastline.

5.2.4 *Quality Control*

Following digitization, the data were checked to make sure that no ice types overlapped, that each ice type was properly identified, and that no slivers or gaps were found in the coverage. The area of each polygon was calculated and each ice shelf and ice tongue was assigned an object identification number that was coded to reveal the relationship between ice features as they calved into different pieces.

The error associated with each observation was determined in two ways. First by considering the resolution of the image used (Ghilani 2000):

$$\sigma_{area} = D\sigma_D \sqrt{2} \quad (5.1)$$

where the uncertainty (σ_{area}) is computed from the equivalent-area square (D), taken as the square root of the area of the polygon, multiplied by the uncertainty in the image (σ_D) or half the spatial resolution. This method has been used by other glaciologists (e.g., Hoffman et al. 2007; Crawford 2013) but it does not account for errors related to delineating ice types or operator error (Crawford 2013; c.f. White and Copland 2015), which were quantified by using four test images (SPOT-1, RADARSAT-1 ScanSAR, RADARSAT-1 Standard Beam and RADARSAT-2 Fine Quad) containing ice shelves

ranging in area from 8.8 to 73 km². These ice shelves were digitized five times on separate occasions to obtain a coefficient of variation that served as a proxy for digitization precision (Paul et al. 2013).

The error estimation using the first method (Ghilani 2000) yielded a relative error of 0.07% for Ward Hunt East Ice Shelf in 2015 using a RADARSAT-2 Fine Quad Beam image, 0.24% for M'Clintock Ice Shelf in 1988 using a SPOT-1 image, 0.29% for Markham Ice Shelf in 2006 using a RADARSAT-1 Standard Beam image, and 1.1% for the same ice shelf but at ScanSAR resolution. The repeat digitization method gave coefficients of variation of 0.04, 0.59, 1.29 and 2.8%, respectively, for these ice shelves. The last image, a ScanSAR RADARSAT-1 image of the Markham Ice Shelf in 2006, had an extent that was on average 6.3% larger than the Standard Beam image, which is a significant difference ($p = 0.001$). This indicates that lower resolution data yield less accurate results but, in this case, the digitization is repeatable within 3%. We found that the relative error derived from the Ghilani (2000) equation was related to the coefficient of variation given by repeat digitization (Adjusted R²: 0.91, $p = 0.03$). Therefore, to estimate the repeatability error (typically the largest error), we multiplied the result of Eq. 5.1 by a factor of 2.54 and added an offset of 0.1%, which yielded an RMSE of 0.26%. For the purposes of generating an error estimate, the 'resolution' of the anecdotal information in 1906 was arbitrarily set at 500 m and the resolution of the scanned maps from 1959 was set at 50 m. All other image resolutions were either the pixel size (optical imagery) or published worst-case resolution for SAR imagery (Table 5.2).

5.3 Results

5.3.1 Overview

Over 2000 ice shelf, ice tongue and ice fragment polygons were digitized over the thirteen observation periods. The original contiguous 'Ellesmere Ice Shelf' in 1906, as recreated from Vincent et al. (2001), was 8597 km² in area (Figs. 5.1 and 5.3a; Table 5.3). In 1959 there were 15 ice shelves with a total area of 2168 km². Then, by 2015 ice shelf extent had decreased by 75% to 535 km² (Table 5.3) distributed among 13 ice shelves (see Fig. 5.2 for current photographs). As ice shelves calved and ice islands moved away from the coast, some feeder glaciers that once merged with ice shelf ice were reclassified from ice shelf to ice tongue (Fig. 5.3b; Table 5.3). This partly offset the loss of ice tongues due to calving. In 1959, there were eight ice tongues with a total area of 94 km². In 2015, there were nine ice tongues with a total area of 23 km² (Table 5.3).

The break-up of ice shelves and glaciers resulted in the production of fragments and ice islands. Most were advected from the study area by a combination of pack ice drift, wind and currents (Sackinger et al. 1985; Jeffries 1992a; Jeffries and Shaw 1993), yet many fragments remained in the fiords and bays. They totalled 9 km² in area in 1959 and 80 km² (mostly in Milne Fiord) in 2015, but with a wide variability

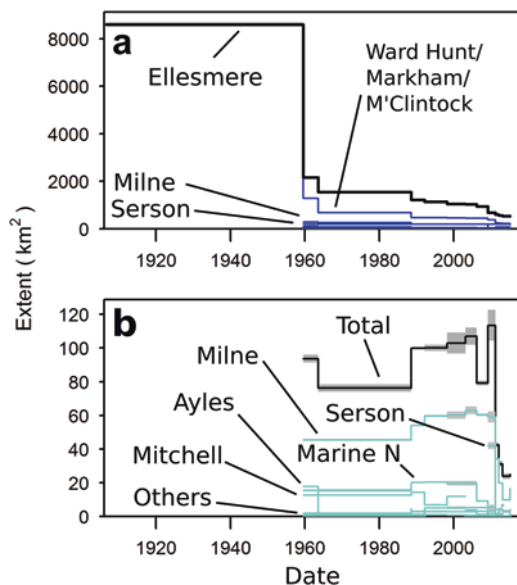


Fig. 5.3 Total and individual extents for (a) ice shelves and (b) ice tongues. The *black line* is the total extent, the thinner coloured lines indicate the extent of individual ice shelves (*dark blue*) or ice tongues (*cyan*). *Grey shading* is the uncertainty in the extent. At this scale, only the large ice shelves are visible. Prominent ice tongues include the Milne, Ayles, Richards North and Fanshawe glaciers (in order of extent). Note that changes in extent are registered only at each of the observation years and do not reflect precise timing of calving events. For example, much of the large ‘Ellesmere Ice Shelf’ likely calved away in the 1930s and 40s, producing large ice islands that were discovered in the 1940s (Belkin and Kessel 2017; Dowdeswell and Jeffries 2017)

Table 5.3 Extent of ice types by year for the northern coast of Ellesmere Island

Year	Ice shelves		Ice tongues		Fragments	
	Area (km ²)	Error (km ²)	Area (km ²)	Error (km ²)	Area (km ²)	Error (km ²)
1906	8597	94.9	–	–	–	–
1959	2168	15.3	94	2.3	9	0.8
1963	1549	20.2	76	2.1	13	1.2
1988	1222	6.4	100	0.7	58	1.6
1992	1143	7.1	100	1.9	49	3.5
1998	1050	18.1	103	6.2	27	3.2
2003	1037	12.6	107	5.2	27	1.7
2006	947	5.1	79	1.5	20	0.7
2009	680	19.6	113	9.2	1	0.6
2011	605	2.5	42	1.5	97	4.9
2012	557	3.2	31	1.8	85	1.1
2013	537	3.4	24	1.7	79	1.7
2015	535	2.2	25	0.2	80	1.3

between years (Table 5.3). The disintegration of ice shelves and ice tongues into fragments as well as their thinning is described below. The following sections give details on each ice shelf that was present in 1959 in order of extent.

5.3.2 *M'Clintock/Ward Hunt/Markham Ice Shelf*

In 1959, the largest remnant of the former Ellesmere Ice Shelf was the contiguous M'Clintock/Ward Hunt/Markham Ice Shelf. Its change in extent since then is documented in Figs. 5.4a and 5.5 as well as Table 5.4. This ice shelf disintegrated over the next several years, losing 598.7 km² in a calving event which created five large ice islands between August 1961 and April 1962, and caused the separation of Ward Hunt/M'Clintock and Markham ice shelves (Hattersley-Smith 1963). The M'Clintock Ice Shelf broke up between August 1963 (Corona imagery, this study) and April 1966 (Hattersley-Smith 1967) and became detached from the Ward Hunt Ice Shelf at that time or soon after (Serson 1983). Between spring 1980 and 1982 a 40 km² loss was estimated near Discovery Ice Rise (Jeffries 1982).

The Ward Hunt Ice Shelf shrank again between June 1982 and April 1983, causing the calving of another ~40 km² of ice islands, including Hobson's Choice Ice Island (Jeffries and Serson 1983; Hobson 1989). No further calving was reported until 2002 when the Ward Hunt Ice Shelf calved ~6 km² of ice, and extensive fracturing resulted in drainage of the epishelf lake in Disraeli Fiord (Mueller et al. 2003). In February 2008, extensive cracks were found over large areas of the eastern part of the Ward Hunt Ice Shelf during an airborne survey and calving occurred that summer (Mueller et al. 2008; Derksen et al. 2012). This isolated two small parts of the ice shelf (Ward Hunt Northwest and North) on the northwest and east side of the Ward Hunt Ice Rise. In August 2010, there was a further calving from the Ward Hunt Ice Shelf to the south and east of Ward Hunt Island that created Ward Hunt East Ice Shelf and left large ice fragments between the two ice shelves (Vincent et al. 2011). This central area disintegrated in 2011 and 2012 along with portions of the Ward Hunt Ice Shelf (Figs. 5.2a, 5.4a and 5.5a).

There is little information about Markham Ice Shelf from 1963 until 1998 since, unlike most of the other ice shelves, no imagery was available in 1988 and 1992. From SAR imagery in the late 1990s it appeared that the ice shelf grew laterally to fill most of the width of the fiord (Figs. 5.4e and 5.5a; Table 5.4). However, the southern edge of the ice shelf moved north over that period. This may have been due to a calving event since some standard beam RADARSAT-1 imagery from 2000 shows what appears to be an ice fragment in the fiord. The southern and western edge of the ice shelf was poorly resolved, particularly in ScanSAR imagery, and variation in ice shelf size may be the result of image interpretation issues. A 2.4 km² calving event along the northern edge of the ice shelf was evident after comparing imagery from 1998 and 2003 (Fig. 5.5a). An examination of ancillary SAR imagery indicated that this calving occurred in 2000. On August 6, 2008, the ice shelf broke up into two main pieces and calved away completely. This event was captured by Moderate Resolution Imaging Spectroradiometer (MODIS) imagery (Mueller et al. 2008).

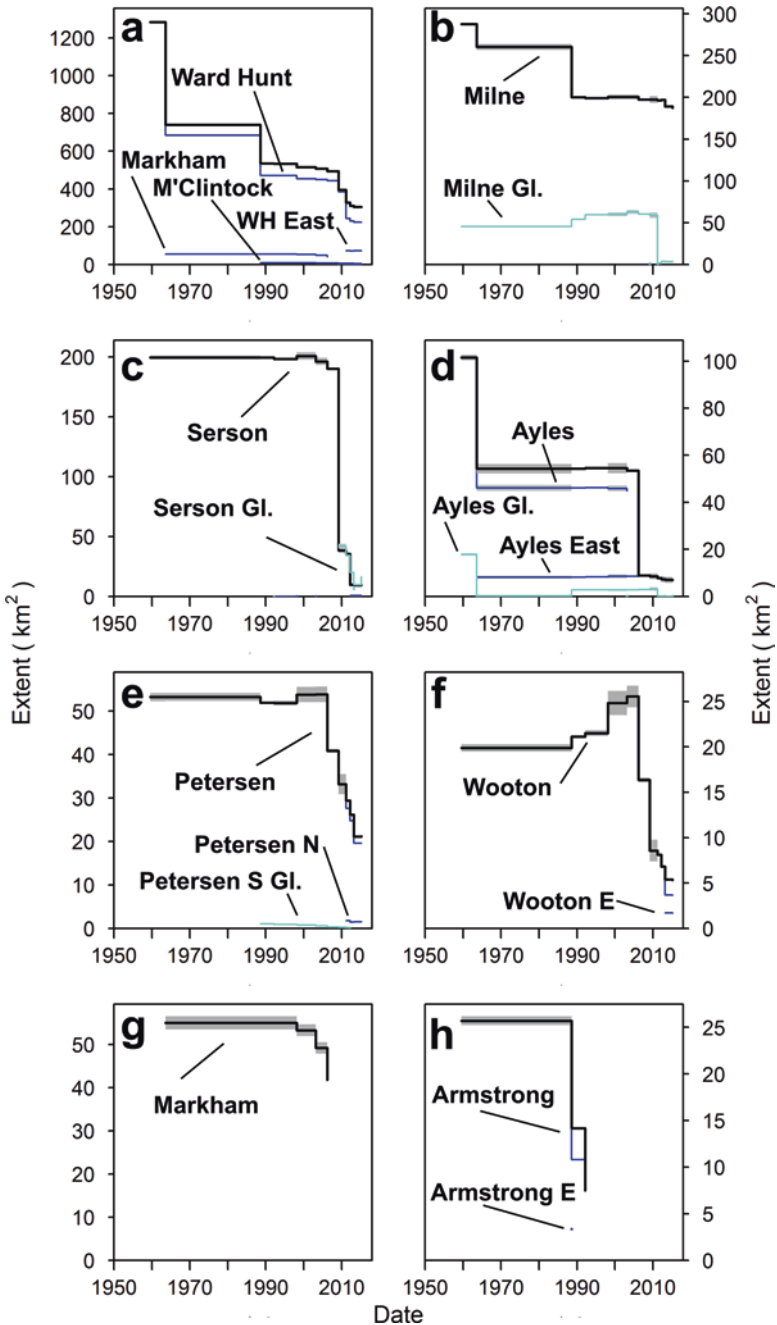


Fig. 5.4 Extents for the following ice shelves and associated ice tongues: (a) M'Clintock/Ward Hunt/Markham, (b) Milne, (c) Serson, (d) Ayles, (e) Petersen, (f) Wooton, (g) Markham, and (h) Armstrong. The *thick black line* is the total extent, the *thinner coloured lines* indicate the extent of individual ice shelves (*dark blue*) and ice tongues (*cyan*) that were created in the disintegration process. *Grey shading* is the uncertainty in the extent. Note that changes in extent are registered only at each of the observation years and do not reflect precise timing of calving events

5.3.3 *Milne Ice Shelf*

In 1959, Milne Fjord was nearly completely covered in thick ice shelf ice from the ice tongue at the head of the fjord to the northern edge of the Milne Ice Shelf at the mouth of the fjord (Fig. 5.6a). A 27 km² calving event at the northern edge of the Milne Ice Shelf (Jeffries 1986a) occurred between 1959 and 1963 as evidenced by the Corona image used in this study (Figs. 5.4b and 5.6a; Table 5.4). Following that calving, little change occurred at the seaward (northern) edge of the ice shelf, but the landward (southern) side changed substantially (Fig. 5.6a).

Jeffries (1986b) defined three regions on the Milne Ice Shelf: the Outer Unit (northernmost third), the Central Unit and the Inner Unit (which abutted against the floating terminus of the Milne Glacier). In 1984, Jeffries (1985) measured the thickness of ice in the Inner Unit to be 3.19 m, which corroborated a thickness of <10 m determined by airborne radio-echo sounding (Prager 1983; Narod et al. 1988). This suggests that the Inner Unit was no longer shelf ice at that time (Mortimer et al. 2012). The area occupied by the Inner Unit (from the 1980s on) is now considered to be an epishelf lake (Mueller et al. 2006; Veillette et al. 2008; Mortimer et al. 2012) with an ice thickness of <2 m measured annually by the authors (Mueller and Copland) between 2008 and 2015. The Central Unit of the Milne Ice Shelf (Fig. 5.2g) also showed regions of smooth, featureless ice which were interpreted as ‘internal’ epishelf lakes starting in 1988 (Fig. 5.6a). These regions of lake ice became even more apparent in SAR imagery owing to their bright radar return (c.f., Jeffries 2002; Veillette et al. 2008; White et al. 2015; Fig. 5.6b), and grew over time in spite of their variable appearance in imagery at times.

Between 2008 (*in situ* observation; Mortimer et al. 2012) and 2009, a straight crack formed across the Central Unit of the ice shelf. This was followed by calving at the southern edge of the ice shelf in late August 2012, when the northwestern third of the epishelf lake ice broke up. There was also extensive break-up within the ice shelf; the southeastern portion of the ice shelf disintegrated in place leaving many small fragments that were not captured by the methods outlined in this study since they did not drift apart appreciably. During 2012–13, a 3 km² portion of ice shelf also calved away near Cape Evans (Figs. 5.4b and 5.6a).

The Milne Glacier tongue also changed considerably over the period 1959–2015 (Figs. 5.4b and 5.6a; Table 5.4). In 1959 the ice tongue was flanked by epishelf lakes on both sides. These increased in size and the glacier advanced (Jeffries 1984; Mortimer 2011) between then and 1988. The ice tongue advanced even further during 1988–2009 and the margins became more deeply and sharply incised by transverse rifts over time. Between 2009 and 2011 the ice tongue calved into the fjord and started to break apart. As of 2015 it was not very cohesive, although it was digitized as several large polygons as most of these pieces are still held in place by epishelf lake ice (Fig. 5.2h).

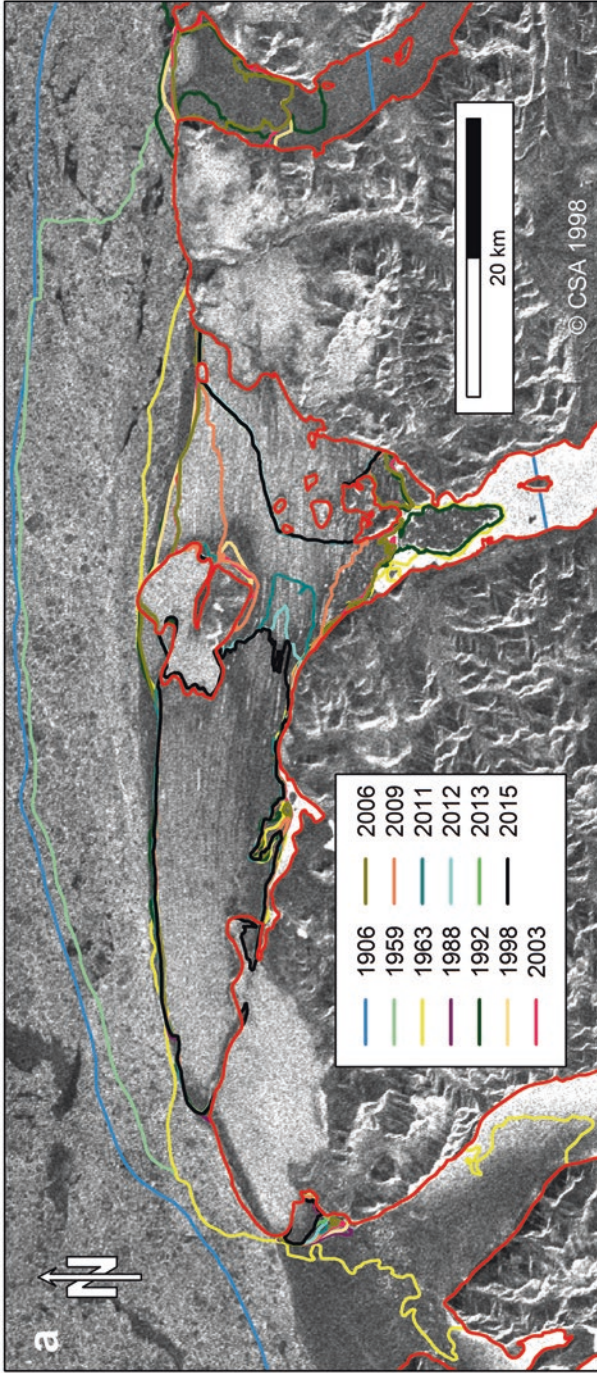


Fig. 5.5 The extent of the Mt. Clintock/Ward Hunt/Markham Ice Shelf (a) from 1959 to 2015 and (b) in 2015. In (a) ice shelf extents are denoted by *coloured lines*; note that the extent in more recent years may cover the extent of previous years. Background images are (a) a RADARSAT-1 ScanSAR HH image acquired on January 13, 1998 and (b) a RADARSAT-2 ScanSAR image acquired on March 22, 2015 (*Red*: HH, *Green* and *Blue*: HV) and two RADARSAT-2 Fine Beam Wide images from March 26, 2015 (*Red*: HH + VH/2, *Blue*: HH + VV), which can be interpreted as the contribution made by the ice targets to single-bounce, volume and double-bounce scattering mechanisms, respectively)

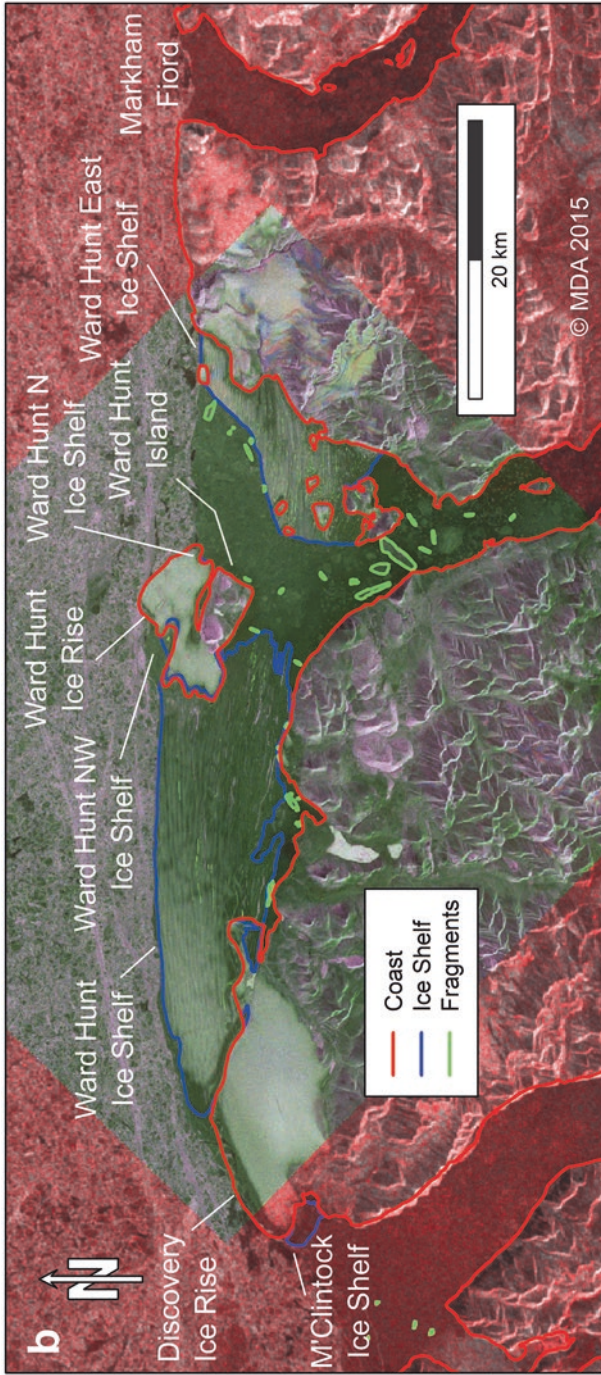


Fig. 5.5 (continued)

Table 5.4 (continued)

Ice feature	1959	1963	1988	1992	1998	2003	2006	2009	2011	2012	2013	2015
Richards Glacier South	0.2	0.2	2.6	2.8	2.8	2.8	2.8	2.8	2.1	2.1	2.1	2.0
Petersen South Glacier	–	–	1.0	0.9	0.8	0.6	0.3	0.3	0.2	0.1	–	–
Serson Glacier	–	–	–	–	–	–	–	42.0	34.1	19.8	16.4	16.6
Total	93.7	76.2	99.8	100.1	102.9	107.0	79.1	113.5	42.3	31.1	23.8	24.9

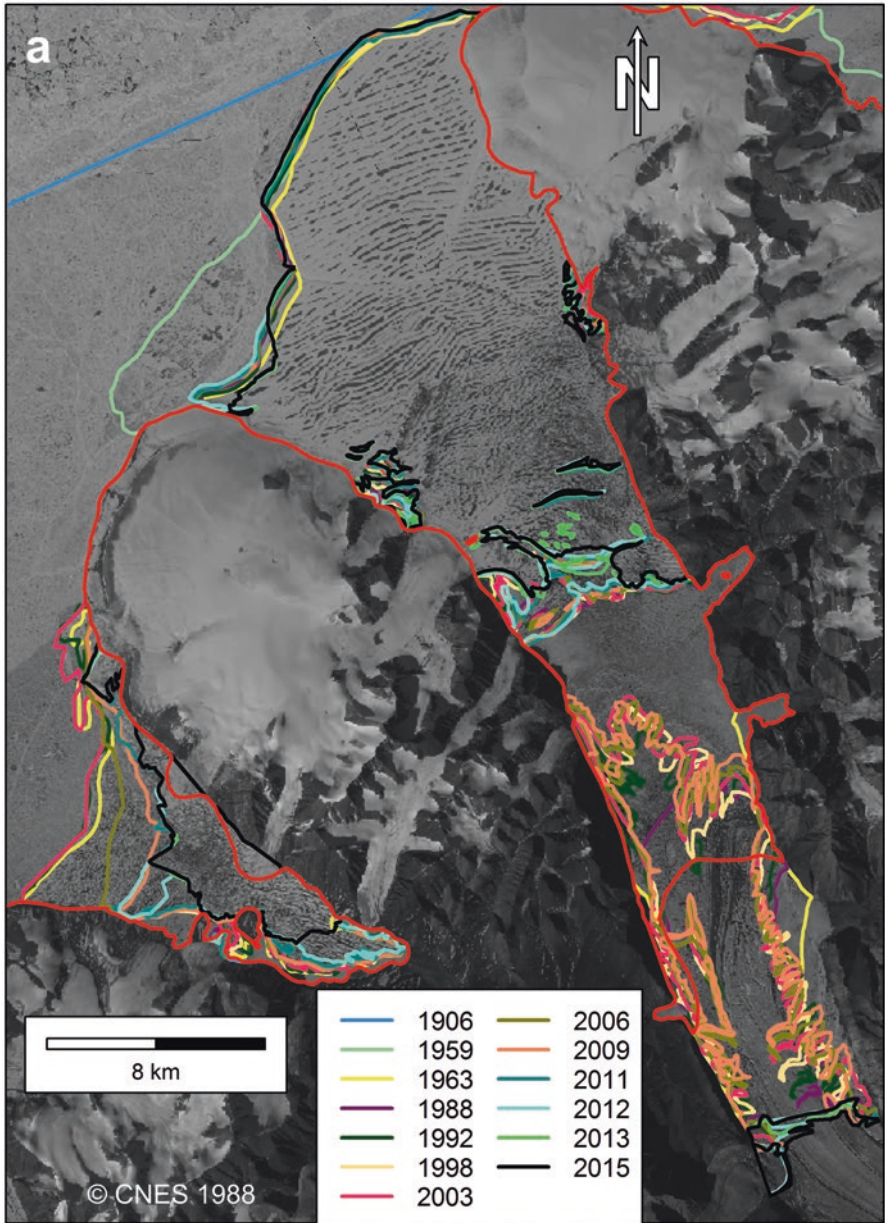


Fig. 5.6 The extent of the Milne and Petersen ice shelves and the Milne Glacier Ice Tongue (a) from 1959 to 2015 and (b) in 2015. In (a) ice shelf and ice tongue extents are denoted by coloured lines; note that the extent in more recent years may cover the extent of previous years. Background images are (a) SPOT-1 true colour multispectral image acquired on August 8, 1988 and (b) two RADARSAT-2 Fine Beam Wide images acquired on March 27, 2015 (Red: HH – VV, Green: (HV + VH)/2, Blue: HH + VV), which can be interpreted as the contribution made by the ice targets to single-bounce, volume and double-bounce scattering mechanisms, respectively)

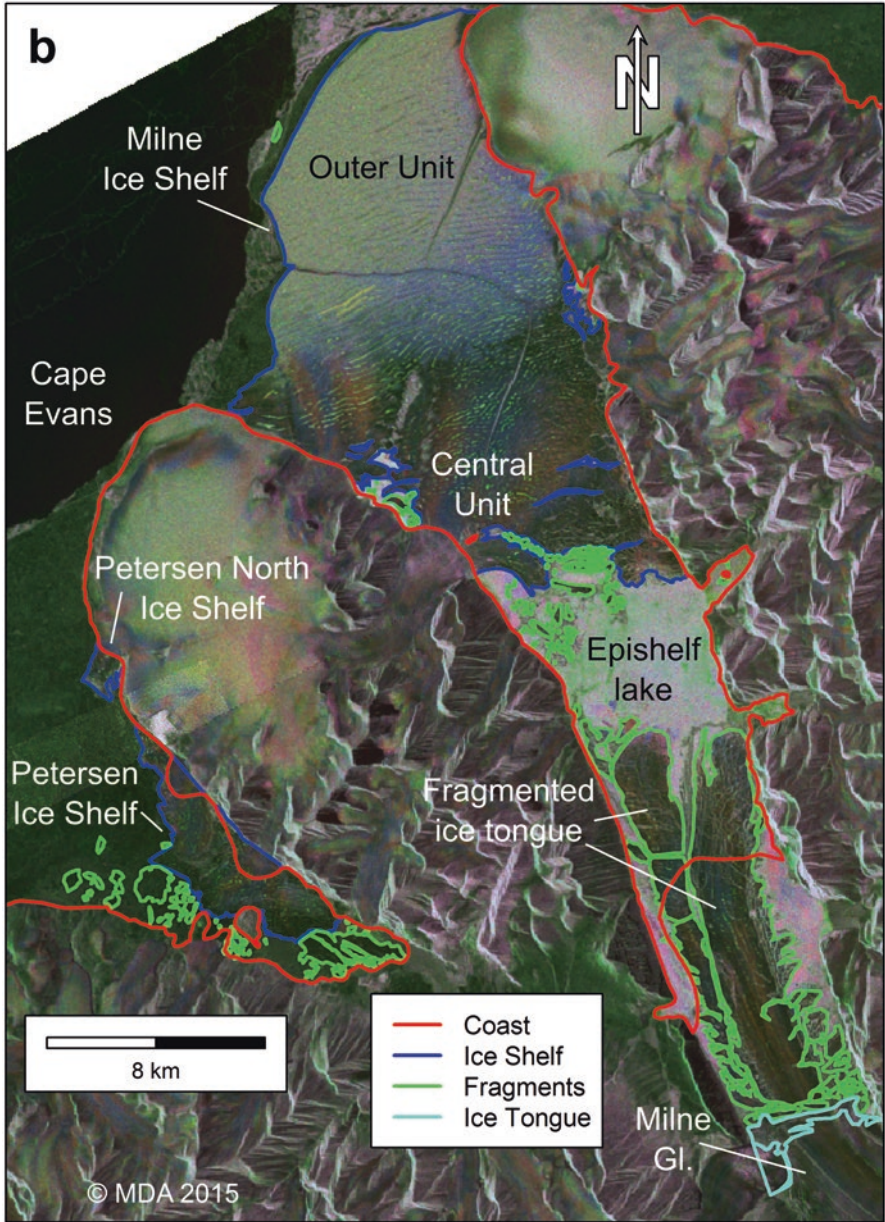


Fig. 5.6 (continued)

5.3.4 *Serson Ice Shelf*

The Serson Ice Shelf was relatively stable from the 1960s until summer 2008, when most of it calved away (Figs. 5.4c and 5.7a; Table 5.4; Mueller et al. 2008). The 1959 map, that was created with data from 1950, suggests a 12 km² greater extent than the polygon we corrected using the aerial photographs from 1959. Much of that discrepancy can be explained by the calving of the ice island ARLIS-II (3 × 6 km) in 1955 (Jeffries 1992b). The Serson Ice Shelf is considered to be a composite of a glacial ice shelf and sea ice ice shelf (Lemmen et al. 1988) and influx of the Serson Glacier (unofficial name) from the southeast appears to have generally compensated for some minor peripheral losses until 2006. There was also continuing development of internal epishelf lakes from at least 1998, particularly in the glacial ice shelf section as well as at the interface between the glacial and sea ice shelf sections (in 2006). This foreshadowed the breaking apart of the two sections of the ice shelf in the summer of 2008 (Mueller et al. 2008).

Following this breakup event, the floating tongue of the Serson Glacier that was, until 2008, an integral part of the ice shelf, was reclassified as ice tongue (Fig. 5.2f). The ice tongue of the glacier to the west of the Serson Glacier calved back, presumably to a grounding line (Fig. 5.7a). The 2008 ice shelf loss of 151 km² (Figs. 5.4c and 5.7a; Table 5.4) can therefore be partitioned into loss of ice extent (110 km²) and reclassification of former ice shelf to ice tongue (41 km²). The ice shelf was further diminished by 26.5 km² between 2011 and 2012 and a small (<1 km²) portion (Serson East) was isolated. The Serson Glacier tongue also lost mass due to calving which was only partially offset by advance during 2008–2015 (Figs. 5.4c and 5.7a; Table 5.4).

5.3.5 *Ayles Ice Shelf*

The Ayles Ice Shelf, with an area of 101 km² in 1959, filled the outer portion of Ayles Fiord past the terminus of a large ice tongue that extended from the glacier at the west side of the fiord (Figs. 5.4d and 5.8a; Table 5.4). Jeffries (1986a) reported that between 1959 and 1974 a 15 km² ice island calved from the Ayles Ice Shelf, and the ice shelf itself detached from the coast and moved seaward 5 km. The Corona image along with aerial photographs (Hattersley-Smith 1967) reveal that these changes actually occurred between 1962 and 1963. At that time, the ice tongue also disintegrated, leaving numerous ice fragments in the fiord. A small portion of the Ayles Ice Shelf remained attached to two coalesced ice tongues in the eastern arm of the fiord. This comprised another smaller ice shelf that was ignored in previous research (e.g., Jeffries 1992a; Mueller et al. 2006). The large portion of the Ayles Ice Shelf (45 km²) that was displaced seaward in the early 1960s remained landfast at the mouth of the fiord until August 2005, when it broke away completely, together with the multiyear landfast sea ice surrounding it (Copland et al. 2007). The Ayles

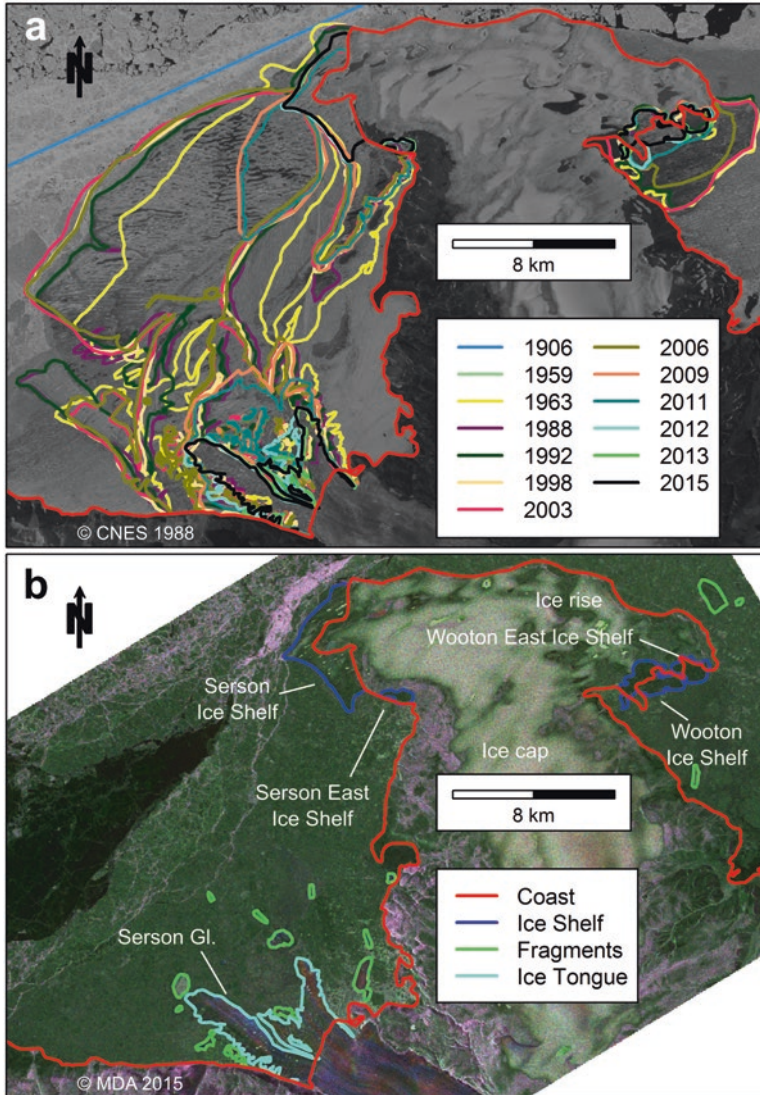


Fig. 5.7 The extent of the Serson and Wooton ice shelves and the Serson Glacier ice tongue **(a)** from 1959 to 2015 and **(b)** in 2015. In **(a)** ice shelf and ice tongue extents are denoted by *coloured lines*; note that the extent in more recent years may cover the extent of previous years. Background images are **(a)** SPOT-1 true colour multispectral image acquired on August 8, 1988 and **(b)** a RADARSAT-2 Fine Beam Wide images acquired on March 24, 2015 (*Red*: HH – VV, *Green*: (HV + VH)/2, *Blue*: HH + VV), which can be interpreted as the contribution made by the ice targets to single-bounce, volume and double-bounce scattering mechanisms, respectively)

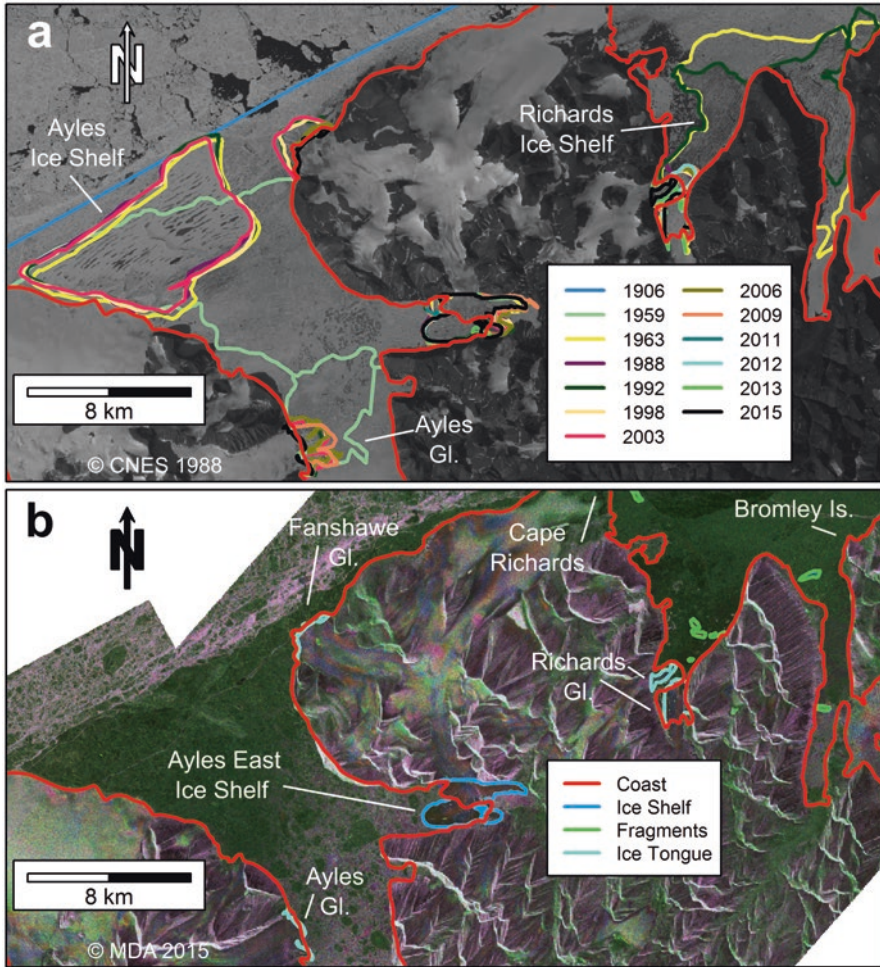


Fig. 5.8 The extent of the Ayles and Richards ice shelves and the Ayles, Fanshawe and Richards glacier ice tongues (a) from 1959 to 2015 and (b) in 2015. In (a) ice shelf and ice tongue extents are denoted by coloured lines; note that the extent in more recent years may cover the extent of previous years. Background images are (a) SPOT-1 true colour multispectral image acquired on August 8, 1988 and (b) a RADARSAT-2 Fine Beam Wide image acquired on March 23, 2015 (Red: $HH - VV$, Green: $(HV + VH)/2$, Blue: $HH + VV$), which can be interpreted as the contribution made by the ice targets to single-bounce, volume and double-bounce scattering mechanisms, respectively)

East Ice Shelf was unaffected by this calving and retained approximately the same extent from 1988 until 2011, before disintegrating slightly (1 km^2) between 2011 and 2015 (Fig. 5.4d). The Ayles Glacier advanced between 1959 and 1988, and again slightly yet continuously between 1998 and 2005, before calving right back to its grounding line in 2012 (Fig. 5.8a; Table 5.4).

5.3.6 *Petersen Ice Shelf*

The extent of the Petersen Ice Shelf was generally stable until the 59–79 year-old multiyear landfast sea ice in Yelverton Bay calved in summer 2005 (Copland et al. 2007; Pope et al. 2012; White et al. 2015), although there was some fluctuation in area with slight growth in the late 1990s (Figs. 5.4e and 5.6a; Table 5.4). After the August 2005 losses there was a marked decline in the ice shelf extent from 2005 to 2012 (White et al. 2015), and continued loss from 2013 to 2015 (Fig. 5.4e). Today, Petersen Ice Shelf consists of two portions, a small ice shelf to the north that separated from the main section between 2009 and 2012 (Fig. 5.6a). The second, main section has since calved to the west into Yelverton Bay (Fig. 5.2c) as well as at the head of Petersen Bay where long ice fragments were formed by fracturing along the east-west trending meltwater lake troughs (Fig. 5.2d). In 2015, most of these fragments remained trapped near the head of the bay behind the main ice shelf (Fig. 5.6b).

5.3.7 *Wooton Ice Shelf*

The Wooton Ice Shelf is located in Yelverton Bay to the east of Serson Ice Shelf (Fig. 5.7). Changes in this ice shelf (1959 to July 2009) were documented by Pope et al. (2012). In this study, the Wooton Ice Shelf was found to have grown in size from 1988 to 2003 because the ice rise to its west took on an ice shelf-like appearance at its margins (Fig. 5.4f). This included the appearance of linear lakes in 1988 and a marked drop in backscatter to a level consistent with the remainder of the ice shelf in SAR imagery. This was followed by a large calving event (a loss of 9 km²) between 2003 and 2006 (Pope et al. 2012) as well as another smaller calving event (1.3 km²) between 2011 and 2012, and yet another in the following year that separated the ice shelf into two sections (Wooton and Wooton East ice shelves; Table 5.4; Fig. 5.2e).

5.3.8 *Other Ice Shelves*

The two westernmost ice shelves in 1959 were found north of Henson Bay and adjacent to Cape Armstrong, respectively, and remained unaltered until 1980 (Serson 1983; Figs. 5.1 and 5.9; Table 5.4). By 1988 the western portion of the Henson Ice Shelf had calved and the Armstrong Ice Shelf broke into two separate ice shelves. There was some further attrition of the Armstrong Ice Shelf in 1992 and then no evidence of the existence of either ice shelf following that (Figs. 5.4h and 5.9; Table 5.4).

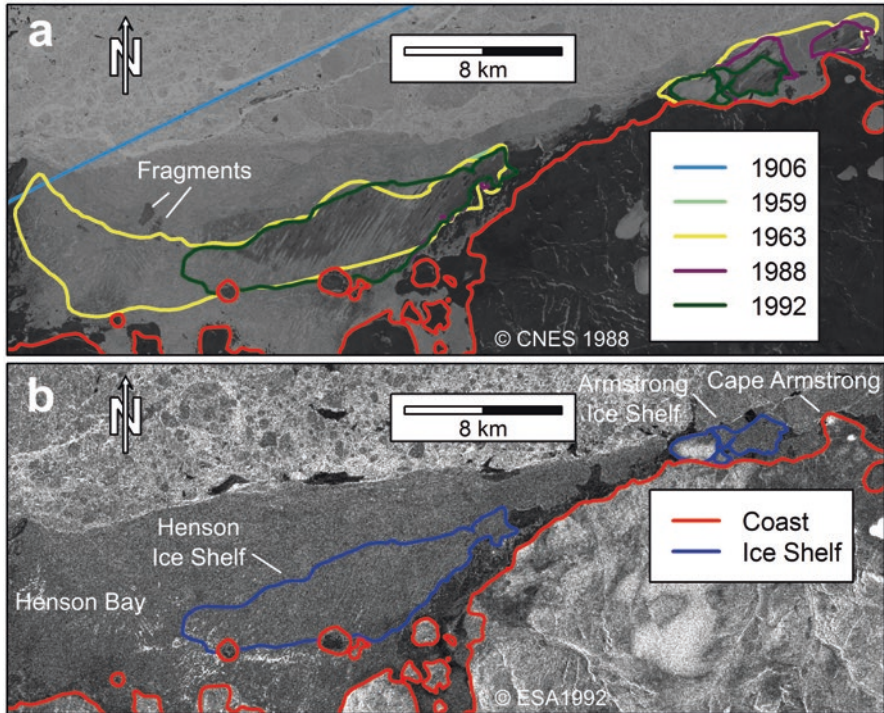


Fig. 5.9 The extent of the Henson and Armstrong ice shelves (a) from 1959 to 1992 and (b) in 1992. In (a) ice shelf extents are denoted by *coloured lines*; note that the extent in more recent years may cover the extent of previous years. Background images are (a) SPOT-1 true colour multispectral image acquired on August 8, 1988 and (b) an ERS-1 Standard Beam HH image acquired on January 24, 1992

Richards Ice Shelf, which occupied the area between Cape Richards and Bromley Island (Fig. 5.8), split in half between 1966 and 1988 (Hattersley-Smith 1967 and SPOT imagery). These two pieces were lost between 1992 and 1998, although two ice tongues which abutted against each other (but didn't appear to merge) remained and then began to disintegrate during the period 2011–2015.

There were two ice shelves, the Columbia Ice Shelf near Markham Ice Shelf and the Aldrich Ice Shelf (both named unofficially after adjacent capes), flanking the main headland of the northernmost coast of Ellesmere Island in 1959 (Fig. 5.10a). These two ice shelves were not imaged between 1963 and 1998 and, although it is difficult to be certain, due to low image contrast, it appears that they both melted or calved away completely during that interval.

To the east of Aldrich Ice Shelf there are four small ice shelves in the embayments to the west of Clements Markham Inlet (Fig. 5.10; Table 5.4). These are named (unofficially) after nearby features (W-E: Doidge Bay, Point Moss, Stuckberry Point and Cape Colan). They were not imaged between 1959 and 1998. Field measurements of ice thickness from 1989–90 indicated that MLSI, not ice

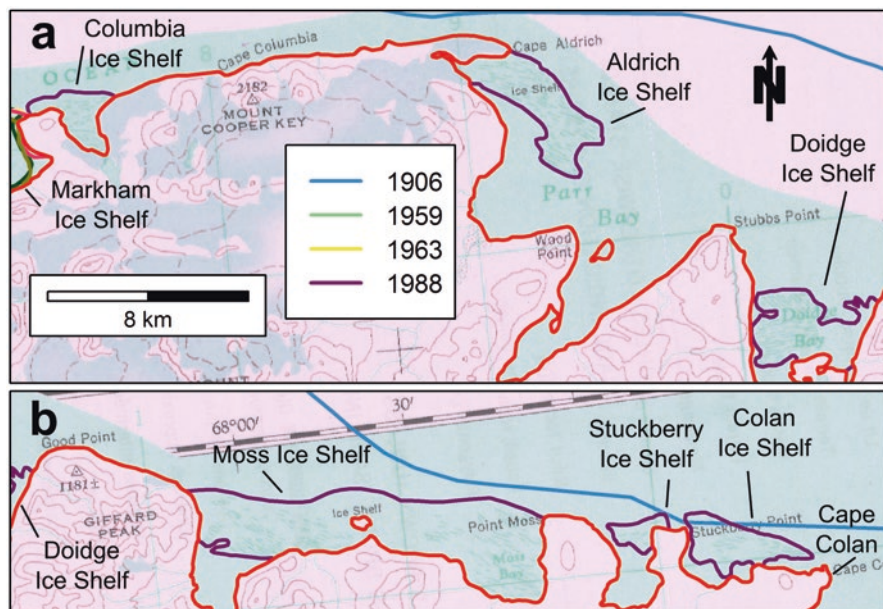


Fig. 5.10 The extent of the (a) Columbia, Aldrich and Doidge ice shelves, as well as the (b) Moss, Stuckberry and Colan ice shelves from 1959 to 1988. Ice shelf extents are denoted by *coloured lines*; note that the extent in more recent years may cover the extent of previous years. Background image is a scan of the Clements Markham (NTS 120F) 1:250,000 map sheet. The scale is the same in both (a) and (b)

shelf ice was present along this coast (Verrall and Todoeschuk unpublished, cited in Jeffries 2017). Furthermore, no ice shelves are apparent in 1998 imagery (Vincent et al. 2001). We therefore assume that these ice shelves thinned away by melting after 1988.

5.4 Discussion

5.4.1 Discoveries and Refinements

In this study, we documented ice shelves and ice tongues along the northernmost coast of Ellesmere Island, and used a systematic approach to digitize their entire but dwindling extent since the start of the twentieth century. As a result, we describe many small ice shelves and ice tongues, some of which were known previously but never properly digitized or described (e.g., Henson, Armstrong and Richards ice shelves along with the ice shelves east of Markham), and other ice shelves which were not recognized by previous researchers (e.g., East Ayles). In addition, large ice tongues such as Serson, Mitchell (south of Wooton Ice Shelf,

not shown) Marine North (south of Petersen Ice Shelf, not shown), Milne, Ayles, Fanshawe and Richards glaciers have now been digitized throughout the entire data record in this project.

While the primary aim of this chapter was to inventory long-term changes in the ice shelves, we have also been able to constrain the timing of some key events with the addition of newly exploited imagery. The Cold War Corona spy satellite helped to refine the timing of calving of the M'Clintock (1963–66), Ayles (1959–63), and Milne (1959–63) ice shelves that have been described in Hattersley-Smith (1967) and Jeffries (1986a), but poorly constrained due to lack of observations. We also discovered new calving events that occurred between the last observation in the published records that end ca. 2009–2012 (Vincent et al. 2011; Pope et al. 2012; Derksen et al. 2012; Mortimer et al. 2012; White et al. 2015) and the winter of 2015. This was the case for Serson, Wooton, Milne (at both the northern and southern calving fronts), Ward Hunt Ice Shelf, East Ayles, and Petersen ice shelves. We also documented calving events that had not previously been recognized in the literature, for example the Markham Ice Shelf calving event that occurred around the turn of the twenty-first century. The recent calving and widespread disintegration of the Milne Glacier tongue has now also been documented, which builds on previous work by Jeffries (1984), Mortimer (2011) and Mortimer et al. (2012).

This work is more comprehensive in terms of spatial and temporal scope than previous studies and, with the exception of studies of single ice shelves (Jeffries 1986a, 1992b; Copland et al. 2007; Mortimer et al. 2012; White et al. 2015), it is also more detailed. For instance, we have delineated small gaps in the extent of ice shelves that had not been fully documented previously, notably on the Serson Ice Shelf, and also on the Milne Ice Shelf (after Mortimer et al. 2012). In conducting this research, we found several places where the disappearance of coastal ice has altered the NTDB 2009 coastline; this was dealt with by identifying and classifying 'inland' polygons to reconcile the difference between this data set and the imagery to properly account for the ice shelf and ice tongue extent within the study area. We did not evaluate more up to date products that are currently available and may have a more accurate coastline. The Government of Canada has not properly mapped the Ellesmere Island ice shelves since the first paper maps of the area were produced in the 1960s (the maps found in the Atlas of Canada were derived from previous versions of this work).

5.4.2 Comparison of Ice Shelf Extents with Previous Literature

In general, the extents that we have calculated are similar to those available in the published literature (Table 5.4). This underscores that the technique we employed along with our interpretation of ice types is repeatable. Percentage differences that are not in bold in Table 5.5 are normally distributed (Shapiro-Wilk $W = 0.96$; $p = 0.48$) and have a mean of 0.22%, suggesting very little systematic bias. The standard

Table 5.5 Comparison between ice shelf extents from this and other studies. Available extents within 5 years of our observation years were included. Values in bold are explained in the text. The Ellesmere Ice Shelf refers to the extent of all ice shelves in 1906 based on anecdotal evidence and the Marvin section is a surveyed subset of this (see Fig. 5.1)

Ice shelf	This study		Other study		Difference (km ²)	Difference (%)	Source	Comments
	Year	Extent (km ²)	Year	Extent (km ²)				
Ellesmere	1906	8529	1906	8900	-371	-4.3	Vincent et al. (2001)	
	1906	8529	1906	7450	1079	12.7	Spedding (1977)	A description of the estimated area is not available
Marvin section	1906	2370	1906	2327	43	1.8	Bushnell (1956)	Table 1 in Vincent et al. (2001)
	1959	1396	1954	1422	-26	-1.9	Crary (1956)	Table 1 in Vincent et al. (2001)
	1963	852	1962	906	-54	-6.3	Hattersley-Smith (1963)	Table 1 in Vincent et al. (2001)
	1988	632	1985	644	-12	-1.9	Jeffries and Serson (1983)	Table 1 in Vincent et al. (2001)
	1998	516	1998	490	26	5.0	Vincent et al. (2001)	Table 1 in Vincent et al. (2001)
Ward Hunt	1988	471	1984	440	31	6.5	Jeffries and Serson (1986)	
Petersen	1988	51.9	early 1980s	55.0	-3.1	-5.9	Jeffries and Serson (1986)	
Wooton	1988	21.1	early 1980s	20.0	1.1	5.4	Jeffries and Serson (1986)	
Serson	2003	200	2000	205	-5	-2.6	Mueller et al. (2006)	
Petersen	2003	53.8	2000	51.2	2.6	4.8	Mueller et al. (2006)	
Milne	2003	200	2001	206	-6	-2.7	Mueller et al. (2006)	
Ayles	2003	46.1	2003	84.1	-38.0	-82.4	Mueller et al. (2006)	Included multiyear landfast sea ice around Ayles Ice Shelf
Ward Hunt	2003	450	2002	448	2	0.5	Mueller et al. (2006)	

(continued)

Table 5.5 (continued)

Ice shelf	This study		Other study		Difference (km ²)	Difference (%)	Source	Comments
	Year	Extent (km ²)	Year	Extent (km ²)				
Markham	2003	49.2	2002	50	-0.8	-1.6	Mueller et al. (2006)	
Ayles	2003	44.8	2005	87.3	-42.5	-94.9	Copland et al. (2007)	Included multiyear landfast sea ice around Ayles Ice Shelf
Milne	1959	288	1959	281	7	2.3	Mortimer et al. (2012)	
	1988	200	1984	250	-50	-25	Mortimer et al. (2012)	Included the epishelf lake
	1992	199	1993	214	-15	-7.5	Mortimer et al. (2012)	
	1998	201	2001	206	-5	-2.5	Mortimer et al. (2012)	
	2009	197	2009	205	-8	-4.1	Mortimer et al. (2012)	
Petersen	1988	51.9	1984	48.4	3.5	6.7	White et al. (2015)	
	1998	53.8	1999	49.9	3.9	7.3	White et al. (2015)	
	2003	53.8	2003	50.3	3.5	6.5	White et al. (2015)	
	2006	40.9	2005	40.8	0.0	0.0	White et al. (2015)	
	2009	33.2	2009	32.1	1.1	3.3	White et al. (2015)	
	2011	27.6	2011	30.3	-2.7	-9.7	White et al. (2015)	
	2012	24.7	2012	24.8	-0.1	-0.4	White et al. (2015)	
	2013	19.6	2012	19.3	0.3	1.4	White et al. (2015)	

deviation is 4.8%, which indicates that the typical discrepancy is within $\pm 5\%$. This aligns well with the worst case uncertainty in digitization (see Sect. 5.2.4). It is difficult to compare two estimates of an extent without any reference to a definitive measurement; however, some of the differences in estimates are discussed below and we suggest reasons for the discrepancies.

The small difference between the original estimate for the Ellesmere Ice Shelf in 1906 and our extent could be due to a difference in geographic projection, digital analysis capability, or a digitizing error. Whatever the source of the error, it is undoubtedly much smaller than the conversion of anecdotal descriptions to a geographical coverage. In particular, Vincent et al. (2001) acknowledged that the

extension of the ice shelves across Nansen Sound to Axel Heiberg Island is controversial. The writings of Otto Sverdrup, who traversed from Ellesmere to Axel Heiberg islands in 1902, indicate the ice was “very much broken and covered with high pressure ridges” (Sverdrup et al. 1904), which is inconsistent with Peary’s description. Koenig et al. (1952) suggest that a large ice island may have occupied Nansen Sound at that time. If this section of the Vincent et al. (2001) ice shelf polygon is excluded, the area of the Ellesmere Ice Shelf was 6373 km² in 1906, which fits better with Spedding’s (1977) estimate of 7450 km², although he also assumed that the ice shelf reached out into Nansen Sound. Unfortunately there are no maps of this reconstruction available to evaluate the differences any further.

Mueller et al. (2006) published the extents of the six largest ice shelves using SAR imagery acquired between 2000 and 2003. These values are within ~5% of the extents obtained here in 2003, with the exception of Ayles Ice Shelf due to the inclusion by Mueller et al. (2006) of multiyear landfast sea ice that grew in around the ice shelf since the 1960s. Copland et al. (2007) had a similar area for the same reasons. Mortimer et al. (2012) included the epishelf lake as part of the Milne Ice Shelf in their 1984 digitization, which explains why our estimate in 1988 is much lower.

5.4.3 *Implications of Semantics*

The 2008 break-up of the Serson Ice Shelf caused this composite ice shelf to become separated into two constituent parts: the sea-ice ice shelf to the north and an ice tongue to the south. The event represented a 151 km² reduction in ice shelf extent, but 27% of this loss was due to the reclassification of parts of the former ice shelf to an ice tongue. For this reason, the scope of this chapter encompasses both thick landfast floating ice types and their break-up products (Table 5.3).

Another related issue is that the operational definition of an ice shelf is based on a minimum thickness. This presents difficulties when thinning reduces an expanse of ice shelf below this threshold. Since the remote sensing data used here don’t quantify thickness, the ice shelf extent can only be gleaned from image interpretation and ancillary information. Interpretation of both optical and SAR data can include judgement of the thickness of ice from the wavelength of surface undulations (c.f. Jeffries and Serson 1986; Jeffries 2017) or by using available ice penetrating radar thickness measurements (Narod et al. 1988; Mortimer et al. 2012; White et al. 2015) or personal observations. It may be useful to consider ice that was formerly ice shelf, but has apparently thinned substantially as ‘transition ice’ (Mortimer 2011; Mortimer et al. 2012). The slow thinning of ice shelves to transition ice was likely the cause of the disappearance of several ice shelves along the northern coast of Ellesmere Island. Examples include Henson, Armstrong and Richards ice shelves along with all the ice shelves east of Markham Ice Shelf. Transition ice is definitely present today at the southeastern margin of Milne Ice Shelf (based on ice penetrating radar observations) and possibly throughout the eastern portion of the Petersen

Ice Shelf (also based on ice penetrating radar, but here reflections were attenuated due to saline ice) (Mortimer et al. 2012; White et al. 2015). Where ice thickness was well constrained, areas of transition ice were removed from the ice shelf extents. However, identifying when those ice areas became too thin to be considered ice shelf ice was a judgement call.

The converse may also be true, where multiyear landfast sea ice may thicken enough to qualify as ice shelf ice. The latter is difficult to explain over the twentieth century, given trends in air temperature and reductions in the average age and thickness of sea ice in the Arctic Ocean, but it may have played a role in some cases (for example, the western side of Markham Ice Shelf). In both cases, we were careful to leverage repeat observations so that the interpretation (thinning or thickening) is consistently applied across the dataset.

5.4.4 Other Known Sources of Data

The collection of ice shelf extents presented here is the most complete to date for anywhere in the Arctic, although it could be improved by incorporating other datasets. This includes using the trimetrogon oblique and vertical photographs taken in 1950, and the original, complete set of vertical air photographs from 1959 that were used to derive the first topographic maps of the region. Also, there is one documented instance where out of date imagery was used to make the map (Jeffries 1992b). There are more air photographs available at the National Air Photograph Library that were taken in 1974 and 1984, although these cover only certain ice shelves and concentrate on their northern edges.

Side-looking airborne real-aperture radar images were obtained in the early 1980s and some airborne X-band SAR images from the late 1980s (Canadian Coast Guard, Canarctic Shipping 1990). For the pre-SAR era, it may also be advantageous to scan and digitize maps from Crary (1954), Hattersley-Smith (1963) and Jeffries and Serson (1983) since they provide fairly detailed reproductions. There are optical satellite data, such as Landsat 5 to 8 imagery and products from the Advanced Spaceborne Thermal Emission and Reflection Radiometer (ASTER) on NASA's Terra satellite, for the more southerly ice shelves (those west of Ayles Fiord). Some high resolution Formosat-2 data exist from the summer of 2008 and there is also relatively good SAR coverage in 1993 (ERS-1), 1997, 2000 and 2008 (RADARSAT-1), and beyond (RADARSAT-2). We recommend that improvements to the current dataset be concentrated on the years before 2003, unless there is a need to better document the timing of individual calving events, in which case the temporal resolution since that date is unparalleled. MODIS optical imagery (250 m resolution) represents a viable option to detect major calving events provided that the imagery is cloud-free, that there is enough contrast between ice shelf and sea ice to detect change, and that fine spatial resolution is not required.

5.4.5 Implications of Ice Shelf Loss

From 1906 to 2015, there has been a monotonic decrease in the extent of the Ellesmere Island ice shelves (Fig. 5.3a; Table 5.3). However, in spite of irregular observations and uncertainty within this dataset, there is evidence of active periods of calving and more quiescent phases. For example, the first half of the twentieth century was a very active period, when 75% of the estimated ice shelf extent in 1906 was lost. In the period from 1959 to 1960 there was also a large loss and a further 30% of the shelf ice calved away. The period following this (1963–1988) saw the loss of ~20% by area of the ice shelves. After these initial years, the pace of loss (in terms of absolute extent lost, relative extent lost and attrition rate) slowed. A relatively quiescent period from the late 1980s to 2003 saw only the loss of 186 km², which was followed by a spate of large calving events in 2005, 2008 and 2010 (Table 5.3; Mueller et al. 2008; Vincent et al. 2011; Derksen et al. 2012). In recent years (since 2012), this rate has slowed again but it will likely increase sporadically in the future (see Copland et al. (2017) for a review on factors that contribute to calving). It is likely that if the rates of attrition in the past 10 years are representative of the future, the remaining Ellesmere Island ice shelves will not last more than 25 years (c.f. White et al. 2015).

The situation for ice tongues is somewhat different, given that they can replenish by ice flow across their grounding lines and their extent varies over time as a result (Fig. 5.3b; Table 5.3). However, ice tongues are also collapsing along the coastline of northern Ellesmere Island (e.g., Milne Glacier; Yelverton Glacier (Adrienne White, unpublished)) and the outlook for the remaining ice tongues is poor.

5.5 Conclusions

The goal of this chapter has been to document the changes of northern Ellesmere Island ice shelves and associated ice tongues since 1906. At present, only 6.3% of the original Ellesmere ice shelf remains, and it seems certain that there will be further attrition and potentially complete loss, in the coming decades. This study has provided the first quantitative assessment of Ellesmere ice shelf disintegration over a century time span with modern GIS and remote sensing techniques. The data are freely available via Nordicana D (Mueller et al. 2017) and can be improved or used for further analyses in the future.

Acknowledgements Corona imagery was acquired through the US Geological Survey's Earth Explorer (<http://earthexplorer.usgs.gov>) and SPOT imagery was obtained courtesy of SPOT Image Corporation. We are indebted to the Alaska Satellite Facility, University of Alaska Fairbanks for providing ERS-1 and RADARSAT-1 imagery from (1992 to 2006). Some supplemental RADARSAT-1 imagery (1998–2006) was accessed through the Polar Data Catalogue (<http://www.polardata.org>). RADARSAT-2 data from 2009 to 2015 were provided by MacDonald, Dettwiler and Associates (MDA) under the RADARSAT-2 Government Data Allocation administered by the Canadian Ice Service (CIS) and the Canadian Space Agency's Science and Operational Applications

Research – Education (SOAR-E) program (project #5054 and #5106). RADARSAT-2 Data and Products are copyright MacDonald, Dettwiler and Associates, Ltd., 2009–2015 – All Rights Reserved. Georeferencing of imagery was conducted in part by Laura Derksen and Mustafa Naziri. Spatial queries and image projections were performed by Sougal Bouh Ali. We are grateful for funding from the Natural Sciences and Engineering Research Council (NSERC), ArcticNet, the Canada Foundation for Innovation, Ontario Research Fund, Ontario Graduate Scholarships, Fonds de recherche du Québec – Nature et technologies (FRQNT) and the Northern Scientific Training Program, and for field support from the Polar Continental Shelf Program. A special thanks to our colleagues and students who have provided insights and valuable discussions over the years, including Adrienne White, Andrew Hamilton, Miriam Richer-McCallum, Sierra Pope and Colleen Mortimer. We also thank Alison Cook and Christian Haas for peer-reviewing this manuscript and providing useful suggestions for improvement.

References

- Aldrich, P. (1877). Western sledge party 1876. In *Journals and proceedings of the Arctic Expedition, 1875–6, under the command of Captain Sir George Nares, R.N., K.C.B. In continuation of Parliamentary Papers C 1153 of 1875 and C 1560 of 1875* (pp. 522). London: Harrison and Sons.
- Antoniades, D. (2017). An overview of paleoenvironmental techniques for the reconstruction of past Arctic ice shelf dynamics. In L. Copland & D. Mueller (Eds.), *Arctic ice shelves and ice islands* (p. 207–226). Dordrecht: Springer. doi:[10.1007/978-94-024-1101-0_8](https://doi.org/10.1007/978-94-024-1101-0_8).
- Belkin, I., & Kessel, S. (2017). Russian drifting stations on Arctic ice islands. In L. Copland & D. Mueller (Eds.), *Arctic ice shelves and ice islands* (p. 367–393). Dordrecht: Springer. doi:[10.1007/978-94-024-1101-0_14](https://doi.org/10.1007/978-94-024-1101-0_14).
- Bushnell, V. C. (1956). Marvin's ice shelf journey, 1906. *Arctic*, 9, 166–177. doi:[10.14430/arctic3791](https://doi.org/10.14430/arctic3791).
- Canadian Coast Guard, Canarctic Shipping. (1990). *Canadian Arctic marine ice atlas – winter 1987/88 with perspectives from 1986/87 and 1988/89*. Ottawa: Canadian Coast Guard.
- Copland, L., Mueller, D. R., & Weir, L. (2007). Rapid loss of the Ayles Ice Shelf, Ellesmere Island, Canada. *Geophysical Research Letters*, 34, L21501. doi:[10.1029/2007GL031809](https://doi.org/10.1029/2007GL031809).
- Copland, L., Mortimer, C. A., White, A., et al. (2017). Factors contributing to recent Arctic ice shelf losses. In L. Copland & D. Mueller (Eds.), *Arctic ice shelves and ice islands* (p. 263–285). Dordrecht: Springer. doi:[10.1007/978-94-024-1101-0_10](https://doi.org/10.1007/978-94-024-1101-0_10).
- Crary, A. P. (1954). Seismic studies on Fletcher's Ice Island, T-3. *EOS, Transactions of the American Geophysical Union*, 35, 293–300.
- Crawford, A. J. (2013). *Ice island deterioration in the Canadian Arctic: Rates, patterns and model evaluation*. MSc thesis, Carleton University, Ottawa.
- De Abreu, R., Arkett, M., Cheng, A., Zagon, T., Mueller, D. R., Vachon, P., & Wolfe, J. (2011). *RADARSAT-2 mode selection for maritime surveillance*. Ottawa: Defence Research and Development Canada.
- Derksen, C., Smith, S. L., Sharp, M., et al. (2012). Variability and change in the Canadian cryosphere. *Climatic Change*, 115, 59–88. doi:[10.1007/s10584-012-0470-0](https://doi.org/10.1007/s10584-012-0470-0).
- Dowdeswell, J. A., & Jeffries, M. O. (2017). Arctic ice shelves: An introduction. In L. Copland & D. Mueller (Eds.), *Arctic ice shelves and ice islands* (p. 3–21). Dordrecht: Springer. doi:[10.1007/978-94-024-1101-0_1](https://doi.org/10.1007/978-94-024-1101-0_1).
- England, J. H., Evans, D. A., & Lakeman, T. R. (2017). Holocene history of Arctic ice shelves. In L. Copland & D. Mueller (Eds.), *Arctic ice shelves and ice islands* (p. 185–205). Dordrecht: Springer. doi:[10.1007/978-94-024-1101-0_7](https://doi.org/10.1007/978-94-024-1101-0_7).
- Flett, D. (2003). Operational use of SAR at the Canadian ice service: Present operations and a look into the future. In *Proceedings of the 2nd Workshop on Coastal and Marine Applications of SAR*, Norway, Svalbard

- Ghilani, C. D. (2000). Demystifying area uncertainty: More or less. *Surveying and Land Information Systems*, 60, 177–182.
- Hattersley-Smith, G. (1957). The rolls on the Ellesmere Ice Shelf. *Arctic*, 10, 32–44. doi:[10.14430/arctic3753](https://doi.org/10.14430/arctic3753).
- Hattersley-Smith, G. (1963). The Ward Hunt Ice Shelf: Recent changes of the ice front. *Journal of Glaciology*, 4, 415–424.
- Hattersley-Smith, G. (1967). Note on ice shelves off the north coast of Ellesmere Island. *Arctic Circular*, 17, 13–14.
- Hobson, G. (1989). Ice island field station: New features of Canadian polar margin. *EOS, Transactions American Geophysical Union*, 70, 833, 835, 838–839.
- Hoffman, M. J., Fountain, A. G., & Achuff, J. M. (2007). 20th-century variations in area of cirque glaciers and glacierets, Rocky Mountain National Park, Rocky Mountains, Colorado, USA. *Annals of Glaciology*, 46, 349–354. doi:[10.3189/172756407782871233](https://doi.org/10.3189/172756407782871233).
- Jeffries, M. O. (1982). The Ward Hunt Ice Shelf, spring 1982. *Arctic*, 35, 542–544. doi:[10.14430/arctic2363](https://doi.org/10.14430/arctic2363).
- Jeffries, M. O. (1984). Milne Glacier, northern Ellesmere Island, N.W.T., Canada: A surging glacier? *Journal of Glaciology*, 30, 251–253. doi:[10.3198/1984JoG30-105-251-253](https://doi.org/10.3198/1984JoG30-105-251-253).
- Jeffries, M. O. (1985). *Physical, chemical and isotopic investigations of Ward Hunt Ice Shelf and Milne Ice Shelf, Ellesmere Island, NWT*. PhD Dissertation, University of Calgary, Calgary.
- Jeffries, M. O. (1986a). Ice island calvings and ice shelf changes, Milne Ice Shelf and Ayles Ice Shelf, Ellesmere Island, N.W.T. *Arctic*, 39, 15–19. doi:[10.14430/arctic2039](https://doi.org/10.14430/arctic2039).
- Jeffries, M. O. (1986b). Glaciers and the morphology and structure of the Milne Ice Shelf, Ellesmere Island, N.W.T., Canada. *Arctic and Alpine Research*, 18, 397–405. doi:[10.2307/1551089](https://doi.org/10.2307/1551089).
- Jeffries, M. O. (1987). The growth, structure and disintegration of Arctic ice shelves. *Polar Record*, 23, 631–649. doi:[10.1017/S0032247400008342](https://doi.org/10.1017/S0032247400008342).
- Jeffries, M. O. (1992a). Arctic ice shelves and ice islands: Origin, growth and disintegration, physical characteristics, structural-stratigraphic variability, and dynamics. *Reviews of Geophysics*, 30, 245–267. doi:[10.1029/92RG00956](https://doi.org/10.1029/92RG00956).
- Jeffries, M. O. (1992b). The source and calving of ice island ARLIS-II. *Polar Record*, 28, 137–144. doi:[10.1017/S0032247400013437](https://doi.org/10.1017/S0032247400013437).
- Jeffries, M. O. (2002). Ellesmere Island ice shelves and ice islands. In R. S. Williams & J. G. Ferrigno (Eds.), *Satellite image atlas of glaciers of the world: North America* (p. J147–J164). Washington, DC: United States Geological Survey.
- Jeffries, M. O. (2017). The ice shelves of northernmost Ellesmere Island, Nunavut, Canada. In L. Copland & D. Mueller (Eds.), *Arctic ice shelves and ice islands* (p. 23–54). Dordrecht: Springer. doi:[10.1007/978-94-024-1101-0_2](https://doi.org/10.1007/978-94-024-1101-0_2).
- Jeffries, M. O., & Sackinger, W. M. (1991). Detection of a calving event at the Milne Ice Shelf, N.W.T. and the contribution of offshore winds. In T. K. S. Murthy, J. G. Paren, W. M. Sackinger, & P. Wadhams (Eds.), *Ice technology for Polar operations* (p. 321–331). Southampton: Computation Mechanics Publications.
- Jeffries, M. O., & Serson, H. V. (1983). Recent changes at the front of Ward Hunt Ice Shelf, Ellesmere Island, N.W.T. *Arctic*, 36, 289–290. doi:[10.14430/arctic2278](https://doi.org/10.14430/arctic2278).
- Jeffries, M. O., & Serson, H. (1986). Survey and mapping of recent ice shelf changes and landfast sea ice growth along the north coast of Ellesmere Island. *Annals of Glaciology*, 8, 96–99.
- Jeffries, M. O., & Shaw, M. A. (1993). The drift of ice islands from the Arctic Ocean into the channels of the Canadian Arctic Archipelago: The history of Hobson's Choice Ice Island. *Polar Record*, 29, 305–312. doi:[10.1017/S0032247400023950](https://doi.org/10.1017/S0032247400023950).
- Jungblut, A. D., Mueller, D., & Vincent, W. F. (2017). Arctic ice shelf ecosystems. In L. Copland & D. Mueller (Eds.), *Arctic ice shelves and ice islands* (p. 227–260). Dordrecht: Springer. doi:[10.1007/978-94-024-1101-0_9](https://doi.org/10.1007/978-94-024-1101-0_9).
- Koenig, L. S., Greenaway, K. R., Dunbar, M., & Hattersley-Smith, G. (1952). Arctic ice islands. *Arctic*, 5, 67–103. doi:[10.14430/arctic3901](https://doi.org/10.14430/arctic3901).

- Lee, J.-S. (2009). *Polarimetric radar imaging: From basics to applications*. Boca Raton: CRC Press.
- Lemmen, D. S., Evans, D. J. A., & England, J. (1988). Ice shelves of northern Ellesmere Island, N.W.T., Canadian landform examples. *Canadian Geographic*, 32, 363–367.
- Mortimer, C. (2011). *Quantification of volume changes for the Milne Ice Shelf, Nunavut, 1950–2009*. Ottawa: University of Ottawa, Department of Geography.
- Mortimer, C. A., Copland, L., & Mueller, D. R. (2012). Volume and area changes of the Milne Ice Shelf, Ellesmere Island, Nunavut, Canada, since 1950. *Journal of Geophysical Research*, 117, F04011. doi:[10.1029/2011JF002074](https://doi.org/10.1029/2011JF002074).
- Mueller, D. R., Vincent, W. F., & Jeffries, M. O. (2003). Break-up of the largest Arctic ice shelf and associated loss of an epishelf lake. *Geophysical Research Letters*, 30, 2031. doi:[10.1029/2003GL017931](https://doi.org/10.1029/2003GL017931).
- Mueller, D. R., Vincent, W. F., & Jeffries, M. O. (2006). Environmental gradients, fragmented habitats and microbiota of a northern ice shelf cryoecosystem, Ellesmere Island, Canada. *Arctic, Antarctic, and Alpine Research*, 38, 593–607. doi:[10.1657/1523-04300](https://doi.org/10.1657/1523-04300).
- Mueller, D. R., Copland, L., Hamilton, A., & Stern, D. R. (2008). Examining Arctic ice shelves prior to 2008 breakup. *EOS. Transactions of the American Geophysical Union*, 89, 502–503.
- Mueller, D., Copland, L., & Jeffries, M. O. (2017). Northern Ellesmere Island ice shelf and ice tongue extent, v. 1.0 (1906–2015). Nordicana D28. doi:[10.5885/45455XD-24C73A8A736446CC](https://doi.org/10.5885/45455XD-24C73A8A736446CC).
- Narod, B. B., Clarke, G. K. C., & Prager, B. T. (1988). Airborne UHF radar sounding of glaciers and ice shelves, northern Ellesmere Island, Arctic Canada. *Canadian Journal of Earth Sciences*, 25, 95–105. doi:[10.1139/e88-010](https://doi.org/10.1139/e88-010).
- Onstott, R. G., & Shuchman, R. A. (2004). SAR measurements of sea ice. In C. R. Jackson & J. R. Apel (Eds.), *Synthetic aperture radar marine user's manual* (p. 81–115). Washington, DC: National Oceanic and Atmospheric Administration.
- Paul, F., Barrand, N. E., Baumann, S., et al. (2013). On the accuracy of glacier outlines derived from remote-sensing data. *Annals of Glaciology*, 54, 171–182. doi:[10.3189/2013AoG63A296](https://doi.org/10.3189/2013AoG63A296).
- Peary, R. E. (1907). *Nearest the pole: A narrative of the Polar expedition of the Peary Arctic club in the S.S. Roosevelt, 1905–1906*. London: Hutchinson.
- Pope, S., Copland, L., & Mueller, D. (2012). Loss of multiyear landfast sea ice from Yelverton Bay, Ellesmere Island, Nunavut, Canada. *Arctic, Antarctic, and Alpine Research*, 44, 210–221. doi:[10.1657/1938-4246-44.2.210](https://doi.org/10.1657/1938-4246-44.2.210).
- Pope, S., Copland, L., & Alt, B. (2017). Recent changes in sea ice plugs along the northern Canadian Arctic Archipelago. In L. Copland & D. Mueller (Eds.), *Arctic ice shelves and ice islands* (p. 317–342). Dordrecht: Springer. doi:[10.1007/978-94-024-1101-0_12](https://doi.org/10.1007/978-94-024-1101-0_12).
- Prager, B. T. (1983). *Digital signal processing of UHF radar system for airborne surveys of ice thicknesses*. Vancouver, BC, Canada: University of British Columbia, Department of Geophysics and Astronomy.
- Ruffner, K. C. (Ed.). (1995). *Corona: America's first satellite program*. Washington, DC: Center for the Study of Intelligence, Central Intelligence Agency.
- Sackinger, W. M., Serson, H. V., Jeffries, M. O., et al. (1985). Ice island generation and trajectories north of Ellesmere Island, Canada. In *Proceedings of the 8th International Conference on Port and Ocean Engineering under Arctic Conditions, Narssarsuaq* (p. 1009).
- Serson, H. V. (1983). *Ice conditions off the north coast of Ellesmere Island, spring 1980*. Victoria: Defence Research Establishment Pacific.
- Shokr, M., & Sinha, N. (2015). *Sea ice: Physics and remote sensing*. Washington, DC: American Geophysical Union.
- Spedding, L. G. (1977). *Ice island count, southern Beaufort Sea 1976*. Calgary: Arctic Petroleum Operations Association.
- Sverdrup, O. N., Bay, E., Schei, P., Simmons, H. G., & Hearn, E. H. (1904). *New land; four years in the Arctic regions*. London: Longmans Green and Co.
- Veillette, J., Mueller, D. R., Antoniadis, D., & Vincent, W. F. (2008). Arctic epishelf lakes as sentinel ecosystems: Past, present and future. *Journal of Geophysical Research – Biogeosciences*, 113, G04014. doi:[10.1029/2008JG000730](https://doi.org/10.1029/2008JG000730).

- Vincent, W. F., Gibson, J. A. E., & Jeffries, M. O. (2001). Ice shelf collapse, climate change, and habitat loss in the Canadian high Arctic. *Polar Record*, *37*, 133–142. doi:[10.1017/S0032247400026954](https://doi.org/10.1017/S0032247400026954).
- Vincent, W. F., Whyte, L. G., Lovejoy, C., Greer, C. W., Laurion, I., Suttle, C. A., Corbeil, J., & Mueller, D. R. (2009). Arctic microbial ecosystems and impacts of extreme warming during the International Polar Year. *Polar Science*, *3*, 171–180. doi:[10.1016/j.polar.2009.05.004](https://doi.org/10.1016/j.polar.2009.05.004).
- Vincent, W. F., Fortier, D., Lévesque, E., Boulanger-Lapointe, N., Tremblay, B., Sarrazin, D., Antoniades, D., & Mueller, D. R. (2011). Extreme ecosystems and geosystems in the Canadian high Arctic: Ward Hunt Island and vicinity. *Ecoscience*, *18*, 236–261. doi:[10.2980/18-3-3448](https://doi.org/10.2980/18-3-3448).
- White, A., & Copland, L. (2015). Decadal-scale variations in glacier area changes across the southern Patagonian Icefield since the 1970s. *Arctic, Antarctic, and Alpine Research*, *47*, 147–167. doi:[10.1657/AAAR0013-102](https://doi.org/10.1657/AAAR0013-102).
- White, A., Copland, L., Mueller, D., & Van Wychen, W. (2015). Assessment of historical changes (1959–2012) and the causes of recent break-ups of the Petersen Ice Shelf, Nunavut, Canada. *Annals of Glaciology*, *56*, 65–76. doi:[10.3189/2015AoG69A687](https://doi.org/10.3189/2015AoG69A687).
- WMO. (1970). *Sea ice nomenclature: Terminology, codes, illustrated glossary and symbols*. Geneva: World Meteorological Organization.